Electronic Supplementary Information for

Heterolytic Cleavage of H_2 by Bifunctional Manganese(I) Complexes: Impact of Ligand Dynamics, Electrophilicity, and Base Positioning

Elliott B. Hulley, Monte L. Helm, R. Morris Bullock*

Center for Molecular Electrocatalysis, Physical Sciences Division, Pacific Northwest National Laboratory, P. O. Box 999, K2-57, Richland, WA 99352, USA

*Correspondence to: morris.bullock@pnnl.gov

Experimental Section

General Considerations

All manipulations were performed in an argon glovebox or via high-vacuum and Schlenk techniques unless otherwise noted. All glassware was oven dried prior to use. Unless otherwise noted, solvents used in syntheses were purified by passing through the neutral alumina columns of an Innovative Technology, Inc., Pure Solv^{TM} purification system, followed by degassing and storage in an argon glovebox over activated 3Å molecular sieves. Hydrogen gas was purified by first passing through two Alltech Oxy-Purge N deoxygenating columns. Infrared spectra were obtained using a Thermo Scientific Nicolet iS10 FTIR spectrometer in a liquid IR cell (CaF_2, International Crystal Laboratories) and samples were prepared under inert atmosphere. $[CPh_3]^+[B(C_6F_5)_4]^-$,[1] $CH_2(PAr^F{}_2)_2$ (bppm),[2] $(P^{Ph}_2N^{Bn}_2)Mn(CO)_3Br$,[3] $(P^{Ph}_2N^{Me})Mn(CO)_3Br$,[3] $(P^{Ph}_2N^{Bn}_2)Mn(Br)(CO)$(bppm),[2] $[(\kappa^3\text{-}P^{Ph}_2N^{Bn}_2)Mn(CO)(bppm)]^+[BAr^F{}_4]^-$,[2] and $[(\kappa^3\text{-}P^{Ph}_2N^{Bn}_2)Mn(CO)(dppm)]^+[BAr^F{}_4]^-$,[3] were prepared according to previously published procedures (Ar^F = 3,5-$(CF_3)_2C_6H_4$). Elemental analyses were performed by Atlantic Microlab in Norcross, Georgia.

NMR Experiments:

Temperatures quoted for NMR experiments are based on calibrations and have an uncertainty of ±0.5 ºC. Deuterium and hydrogen deuteride (HD) were purchased from Sigma Aldrich and used as received. NMR spectra were obtained on a Varian 500 MHz (INOVA or VNMRS) or 300 MHz (VNMRS) spectrometer. ^{1}H NMR chemical shifts were referenced relative to the residual monoprotio solvent (for deuterated solvents) or 5.32 ppm for CH_2Cl_2. ^{13}C NMR chemical shifts recorded in CD_2Cl_2 were referenced relative to CD_2Cl_2 at 53.84 ppm. ^{1}H NMR spectra recorded in CH_2Cl_2 were subjected to wet1d solvent suppression prior to acquisition. ^{2}H NMR spectra recorded in CH_2Cl_2 were referenced relative to a spike of CD_2Cl_2 (~5% v/v) at 5.32 ppm. ^{19}F NMR spectra were referenced to $CFCl_3$ at δ = 0 using the *setref* command in VNMRJ. ^{31}P NMR spectra were proton decoupled unless otherwise stated, and chemical shifts were referenced to external phosphoric acid. ^{15}N NMR spectra were proton decoupled unless otherwise stated, and chemical shifts were referenced to $CH_3{}^{15}NO_2$ at δ = 0

using the *setref* command in VNMRJ. Second-order spectra were simulated using a non-linear regression routine implemented in the gNMR software package; reported coupling constants were extracted from these simulations. Deuterated NMR solvents were purchased from Cambridge Isotopes Laboratories and dried over P_2O_5 for a week under N_2 and vacuum distilled through a glass wool plug.

Syntheses

$(P^{Ph}_2N^{Me})Mn(H)(CO)_3$

To a 100 mL Schlenk flask was added $(P^{Ph}_2N^{Me})Mn(Br)(CO)_3$ (628 mg, 1.28 mmol) and 40 mL THF. Lithium aluminum hydride (164 mg, 4.3 mmol, 3.4 eq) was added in small portions while vigorously stirring the solution; gas evolution was observed. After stirring for ~18h the solution was quenched with deoxygenated, distilled water until evolution of H_2 ceased (ca. 100 μL). The solvent was removed *in vacuo* and the residual beige solid was suspended in PhF and filtered through a pad of Celite on a filter frit. The solvent was removed from the filtered solution *in vacuo* to yield 371 mg off-white powder (70%). ^{1}H NMR (CD_2Cl_2): δ 7.74 (m, 2H, PhH); 7.72 (m, 2H, PhH); 7.37 (m, 12H, PhH); 3.46 (dd, J_{HH} = 13.6 Hz, J_{PH} = 4.4 Hz, 2H, PNP CH_2); 2.72 (d, J = 13.6 Hz, 2H, PNP CH_2); 2.50 (s, 3H, CH_3); –7.36 (t, J_{PH} = 46.4 Hz, 1H, MnH). ^{31}P NMR (CD_2Cl_2): δ 50.2 (d, J_{PH} = 46.4 Hz). IR (PhF): 2000 cm^{-1} (ν_{CO}), 1921 cm^{-1} (ν_{CO}), 1901 cm^{-1} (broad, ν_{CO}). Anal. Calc for $C_{30}H_{28}MnNO_3P_2$: C, 63.50; H, 4.97; N, 2.47;. Found: C, 63.57; H, 5.12; N, 2.58.

$(P^{Ph}_2N^{Me})Mn(OTf)(CO)_3$

A 20 mL scintillation vial was charged with $(P^{Ph}_2N^{Me})MnH(CO)_3$ (50 mg, 0.09 mmol) and 4 mL PhF. While stirring vigorously, silver trifluoromethanesulfonate (22 mg, 1 eq.) was added. Over the course of a minute the white suspension became a cloudy yellow solution with a visible brown/black precipitate. After stirring 16 h the solution was filtered through a PTFE syringe filter and the solvent was removed *in vacuo*, yielding a yellow microcrystalline powder (45 mg, 71%). ^{1}H{^{31}P} NMR (CD_2Cl_2): δ 7.59 (d, J_{HH} = 7.7 Hz, 4H, *o*-Ph^a-H); 7.51 (d, J_{HH} = 7.7 Hz, 4H, *o*-Ph^b-H); 7.48(t, J_{HH} = 7.7 Hz, 2H, *p*-Ph^a-H); 7.41 (t, J_{HH} = 7.7 Hz, 4H, *m*-Ph^a-H); 7.39 (t, J_{HH} = 7.7 Hz, 2H, *o*-Ph^b-H); 7.31 (t, J_{HH} = 7.7 Hz, 4H, *m*-Ph^b-H). ^{19}F NMR (CD_2Cl_2): δ –75.67 (s). ^{31}P

NMR (CD_2Cl_2): δ 25.2 (s). IR (PhF): 2041 cm^{-1} (ν_{CO}), 1974 cm^{-1} (ν_{CO}), 1932 cm^{-1} (ν_{CO}). Anal. Calc for $C_{43}H_{37}F_5MnNO_6P_2S$: C, 56.90; H, 4.11; N, 1.54. Found: C, 56.16; H, 3.99; N, 1.55.

($P^{Ph}_2N^{Me}$)Mn(Br)(CO)(bppm)

A 100 mL Schlenk flask (Pyrex) was charged with ($P^{Ph}_2N^{Me}$)Mn(Br)$(CO)_3$ (631 mg, 1.30 mmol), bppm (1.48 g, 1.2 eq.), and 50 mL PhF. The bppm ligand appears to reversibly convert to an unknown compound possessing a broad ^{31}P resonance around –20 ppm under photolysis conditions; addition of $NaBAr^F$ seems to convert this material back to bppm. In order to facilitate the addition of bppm to ($P^{Ph}_2N^{Me}$)Mn(Br)$(CO)_3$, catalytic $NaBAr^F$ (~5 mg, 0.5 mol %) was added to the flask. The resulting yellow slurry was irradiated by a medium-pressure Hg lamp (Hanovia) for 2 h under N_2 purge with rapid stirring. Halfway through the reaction the progress was checked by ^{31}P NMR spectroscopy, and the solvent lost due to evaporation was replenished. Upon completion (>90% conversion), the solvent was removed *in vacuo* and the resulting red semisolid was dissolved in a mixture of hexane and PhF (~2:1) and filtered through Celite to remove some of the excess bppm. The solvent was removed under vacuum to yield a red solid, which was subsequently dissolved in toluene and crystallized from toluene:hexane (~2:1) at –78 ºC to yield 209 mg (0.127 mmol, 10 %) of the crystalline toluene solvate. The low isolated yield is largely due to the difficulty in separation of the product from residual bppm; as bppm seems inert to subsequent steps, crude ($P^{Ph}_2N^{Me}$)Mn(Br)(CO)(bppm) can be used to make ($P^{Ph}_2N^{Me}$)Mn(H)(CO)(bppm), which can be more readily isolated. The C_s-symmetry of the molecule requires that there are two distinct Ph environments on the PNP ligand (top and bottom); these are denoted 'Ph^a' and 'Ph^b' in the ^1H NMR spectral data. $^1H\{^{31}P\}$ NMR (CD_2Cl_2): δ 7.92 (s, 2H, *p*-Ar^F); δ 7.90 (s, 4H, *o*-Ar^F); δ 7.85 (s, 2H, *p*-Ar^F); δ 7.68 (s, 4H, *o*-Ar^F); δ 7.46 (d, *J* = 7.7 Hz, 4H, *o*-Ph^a-H); δ 7.28 (t, *J* = 7.3 Hz, 2H, *p*-Ph^b-H); δ 7.21 (d, *J* = 8 Hz, 2H, *o*-Ph^b-H); δ 7.09 (m, 6H, *p*-Ph^a-H + *m*-Ph^b-H); δ 6.90 (t, *J* = 7.6 Hz, 4H, *m*-Ph^a-H); δ 4.88 (d, *J* = 14.8 Hz, 1H, bppm C*H*H); δ 4.53 (d, *J* = 14.8 Hz, 1H, bppm CH*H*); δ 4.22 (d, *J* = 12.8 Hz, 1H, PNP C*H*H); δ 3.23 (d, *J* = 12.8 Hz, 2H, PNP CH*H*); δ 2.34 (s, 3H, NCH_3). ^{31}P NMR (CD_2Cl_2): δ 38.8 (br. s, PNP); δ 21.9 (br. s, bppm). ^{19}F NMR (CD_2Cl_2): δ –63.85 (s, 12F, bppm CF_3); δ –63.90 (s, 12F, bppm CF_3). IR (PhF): 1836 cm^{-1} (ν_{CO}). Anal. Calc. for $C_{70}H_{55}BrF_{24}MnNOP_4$: C, 50.70; H, 3.07; N, 0.87. Found: C, 50.63; H, 3.23; N, 0.96.

$(P^{Ph}_2N^{Me})Mn(H)(CO)(bppm)$

A 50 mL Schlenk flask was charged with $(P^{Ph}_2N^{Me})Mn(Br)(CO)(bppm)$ (300 mg, 0.22 mmol), $NaB(Ar^F)_4$ (285 mg, 0.32 mmol, 1.5 eq.), and 15 mL PhF. The solution was degassed and H_2 (1.4 atm) was admitted to the flask while stirring. The solution was stirred for 44 hours, replenishing the H_2 atmosphere mid-way, during which time the solution color changed from red to yellow-orange. N,N-diisopropylethylamine (200 μL, 1.1 mmol, 3.6 eq.) was added, resulting in a color change to deep red, and after 1.5 hr the solvent was removed *in vacuo* and the resulting solid was washed with hexanes (5 × 20 mL) to yield 213 mg crude product. This material could be recrystallized from toluene/hexane and, after washing with pentane, yielded 93 mg (33%) of red crystals. $^1H\{^{31}P\}$ NMR (CD_2Cl_2): δ 8.00 (s, 4H, *o*-Ar^F); δ 7.81 (s, 2H, *p*-Ar^F); δ 7.76(s, 2H, *p*-Ar^F); δ 7.57 (d, J_{HH} = 7.5 Hz, 4H, *o*-Ph^a-H); δ 7.49 (s, 4H, *o*-Ar^F); δ 7.22 (t, J_{HH} = 7.5 Hz, 2H, *p*-Ph^a-H); δ 7.08 (t, J_{HH} = 7.5 Hz, 4H, *m*-Ph^a-H); δ 6.98 (t, J_{HH} = 7.5 Hz, 2H, *p*-Ph^b-H); δ 6.95 (d, J_{HH} = 7.5 Hz, 4H, *o*-Ph^b-H); δ 6.88 (t, J_{HH} = 7.5 Hz, 4H, *m*-Ph^b-H); δ 4.49 (d, J_{HH} = 14 Hz, 1H, bppm C*H*H); δ 4.08 (dd, J_{HH} = 14 Hz, 7 Hz; 1H, bppm CH*H*); δ 3.47 (d, J_{HH} = 12.9 Hz, 2H, PNP C*H*H); 3.42 (d, J_{HH} = 12.9 Hz, 2H, PNP CH*H*); 2.24 (s, 3H, NCH_3); –3.47 (d, J_{HH} = 7 Hz, 1H, Mn*H*). ^{31}P NMR (CD_2Cl_2): δ 62.1 (m, bppm); δ 52.3 (m, PNP). ^{19}F NMR (CD_2Cl_2): δ –63.22 (s, 12F, bppm CF_3); δ –63.36 (s, 12F, bppm CF_3). IR (PhF): cm^{-1} (ν_{CO}). Anal. Calc for $C_{61}H_{42}F_{24}MnNOP_4$: C, 50.89; H, 2.94; N, 0.97. Found: C, 50.96; H, 3.00; N, 1.03.

$[(P^{Ph}_2N^{Me})Mn(CO)(bppm)][B(C_6F_5)_4]$

A 5 mL round bottom flask was charged with $(P^{Ph}_2N^{Me})Mn(H)(CO)(bppm)$ (50 mg, 35 mmol) and $[CPh_3][B(C_6F_5)_4]$ (33 mg, 1.0 eq.). A 180º metered vacuum adaptor was affixed to the flask and the assembly was evacuated on the high-vacuum line ($<10^{-4}$ torr). The flask was cooled to –78 ºC and PhF (~3 mL) was condensed into the flask. The suspension was stirred as it was allowed to warm to 22 ºC over several minutes, and there was a color-change from red to blue-green. After stirring for 1h the solution was degassed and then allowed to stir for a further 18h. The solvent was removed under vacuum, the blue residue was washed with ~ 1 mL PhF in the glovebox, and then the solid was dried under vacuum to yield 33.4 mg (50 mmol, 45%) of blue microcrystals. IR (nujol, crystals of κ^2-isomer): 1854 cm^{-1} (ν_{CO}). Anal. Calc for $C_{85}H_{43.5}BF_{44.5}MnNO_2P_4$: C, 47.58; H, 2.04; N, 0.65. Found: C, 47.53; H, 1.99; N, 0.64.

[(κ^3-$P^{Ph}_2N^{Bn}_2$)Mn(CO)$_3$][BAr^F]

A 20 mL scintillation vial was charged with ($P^{Ph}_2N^{Bn}_2$)Mn(CO)$_3$Br (78 mg, mmol) and 2 mL PhF. To this yellow solution was added NaBAr$^F_4$ (121 mg, 1.2 eq.) and the solution was stirred for 18h. The suspension was filtered through a PTFE syringe filter and the solvent was removed *in vacuo* yielding a yellow residue. This residue was suspended in CH_2Cl_2, refiltered through a PTFE syringe filter, and the solvent removed *in vacuo* to yield a yellow foam. The foam was crushed to a yellow powder and dried under vacuum for 4 h (mg, %). $^1H\{^{31}P\}$ NMR (CD_2Cl_2): δ 7.71 (m, 10H, *m*-BAr^F + Ph-H); 7.63 (t, J_{HH} = 7.5 Hz, 4H, Ph-H); 7.55 (s, 4 H, *p*-BAr^F); 7.51 (d, J_{HH} = 7.5 Hz, 4H, Ph-H); 7.47 (t, J_{HH} = 7.3 Hz, 2H Ph-H); 7.36 (m, 4H, Ph-H); 7.23 (d, J_{HH} = 7.5 Hz, 4H, Ph-H); 4.81 (d, J_{HH} = 14 Hz, 2H, P_2N_2 CH_2); 4.78 (d, J_{HH} = 14 Hz, 2H, P_2N_2 CH_2); 3.91 (s, 2H, Bn CH_2); 3.66 (d, J_{HH} = 14 Hz, 2H, P_2N_2 CH_2); 3.60 (s, 2H, Bn CH_2); 3.40 (d, J_{HH} = 14 Hz, 2H, P_2N_2 CH_2). ^{31}P NMR (CD_2Cl_2): δ –3.5 (s, P_2N_2). IR (PhF): 2041 cm^{-1} (ν_{CO}), 1974 cm^{-1} (ν_{CO}), 1952 cm^{-1} (ν_{CO}). Anal. Calc for $C_{65}H_{45}BF_{24}MnN_2O_3P_2$: C, 52.55; H, 3.05; N, 1.89. Found: C, 53.17; H, 3.17; N, 2.13.

NMR Tube Experiments.

[($P^{Ph}_2N^{Me}$)Mn(CO)$_2$(bppm)][B(C$_6$F$_5$)$_4$]

A resealable NMR tube was charged with [($P^{Ph}_2N^{Me}$)Mn(CO)$_2$(bppm)][B(C$_6$F$_5$)$_4$] (5 mg, 2 μmol) and PhF (0.5 mL). The tube was connected to a vacuum-line, degassed, and CO (0.5 atm) was admitted. Upon shaking the tube there was an immediate color change to yellow as the mostly insoluble [($P^{Ph}_2N^{Me}$)Mn(CO)$_2$(bppm)][B(C$_6$F$_5$)$_4$] dissolved to produce a clear solution. The solvent was removed under vacuum, producing a yellow solid, which was redissolved in CD_2Cl_2 for NMR spectroscopy. IR (PhF): 1907 cm^{-1} (ν_{CO}). ^1H NMR (CD_2Cl_2): δ 8.11 (s, 4H, *p*-Ar^F); δ 7.57 (s, 8H, *o*-Ar^F); δ 7.43 (t, J_{HH} = 7.5 Hz, 4H, *p*-Ph-H); δ 7.22 (t, J_{HH} = 7.5 Hz, 8H, *m*-Ph-H); δ 7.13 (d, J_{HH} = 7.5 Hz, 8H, *o*-Ph-H); δ 4.51 (s, 2H, bppm C*H*$_2$); 3.54 (s, 4H, PNP C*H*$_2$); 2.49 (s, 3H, NC*H*$_3$). ^{31}P NMR (CD_2Cl_2): δ 36.1 (m); δ 34.4 (m). ^{19}F NMR (CD_2Cl_2): δ –63.97 (s, 24F, bppm CF_3) δ –133.75 (s, 8F, *o*-C_6F_4-F); δ –164.33 (s, 4F, *p*-C_6F_4-F); δ –168.12 (s, 8F, *o*-C_6F_4-F).

[($P^{Ph}_2N^{Me}$(H))MnH(CO)(bppm)][$B(C_6F_5)_4$].

A resealable NMR tube was charged with [($P^{Ph}_2N^{Me}$)Mn(CO)(bppm)][$B(C_6F_5)_4$] (~10 mg, 5 μmol) and PhF (mL). A small septum was affixed to the resealable connection, the tube and headspace were degassed *in vacuo* and H_2 (1.4 atm) was admitted *via* needle through the septum and valve. Upon shaking the tube there was an immediate color change to blue-green to yellow-orange as the mostly insoluble [($P^{Ph}_2N^{Me}$)Mn($CO)_2$(bppm)][$B(C_6F_5)_4$] dissolved to produce a clear solution. $^1H\{^{31}P\}$ NMR (–52 ºC, PhF, aryl region partially obscured by wet1d solvent suppression): δ 8.01 (s, 4H, *o*-Ar^F); δ 7.59 (s, 4H, *o*-Ar^F); δ 7.56 (s, 2H, *p*-Ar^F); δ 7.50 (s, 2H, *p*-Ar^F); δ 4.39 (d, J_{HH} = 12 Hz, 1H, bppm C*H*H); δ 4.25 (s, 1H, N*H*); δ 4.10 (br. s., 2H, PNP C*H*H); δ 3.78 (d, J_{HH} = 12 Hz; 1H, bppm CH*H*); δ 3.62 (d, J_{HH} = 12 Hz, 2H, PNP CH*H*); 2.63 (s, 3H, NCH_3); –3.46 (br s, 1H, Mn*H*). ^{31}P NMR (–31 ºC, PhF): δ 73.5 (m, PNP), δ 50.0 (m, bppm).

Figure S1. Solid-state Structure of ($P^{Ph}N^{Me}P^{Ph}$)Mn(OTf)$(CO)_3$ (5-OTf)

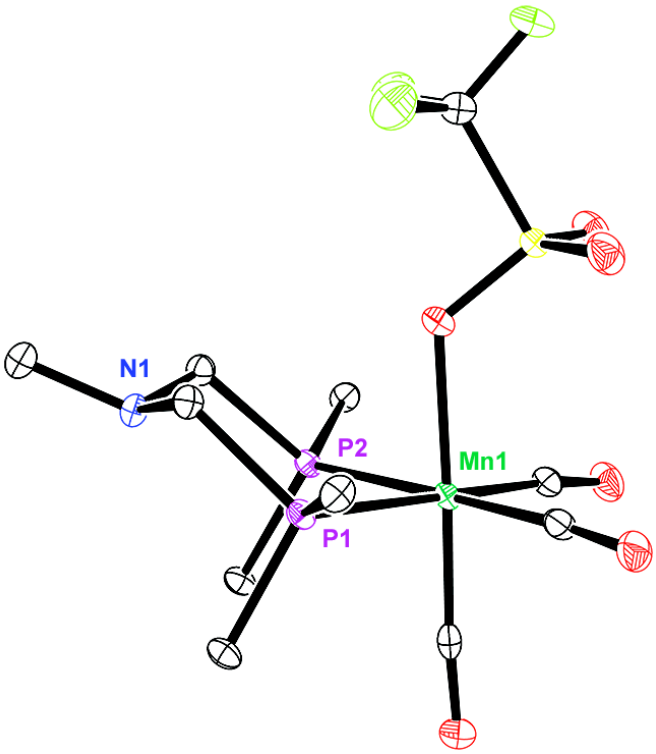

Solid-state molecular structures of ($P^{Ph}N^{Me}P^{Ph}$)Mn(OTf)$(CO)_3$ (**5-OTf**, at –173 °C). Substituents on the P and N have been truncated, and hydrogen atoms and co-crystallized PhF have been omitted for clarity.

Table S1: Selected Distances and Angles in $2[\kappa^3]^+$ and $3[\kappa^3]^+$.

Selected Bond Distances (Å) and Angles (°) for cations $2[\kappa^3]^+$ and $3[\kappa^3]^+$.		
	$2[\kappa^3]^+$	$3[\kappa^3]^+$
Mn-P1	2.214(1)	2.228(1)
Mn-P2	2.244(1)	2.244(1)
Mn-P3	2.318(1)	2.277(1)
Mn-P4	2.307(1)	2.287(1)
Mn-N1	2.316(3)	2.290(2)
P1-Mn-P2	84.79(4)	86.17(2)
P2-Mn-P3	98.56(4)	101.62(2)
P3-Mn-P4	72.51(3)	72.89(2)
P4-Mn-P1	101.98(4)	98.39(2)
P2-Mn-P4	166.43(4)	170.26(2)
P1-Mn-P3	168.13(4)	169.61(2)
N1-Mn-CO	158.1(1)	158.10(8)

Figure S2. Variable Temperature $^{31}P\{^{1}H\}$ NMR Spectra of $3[\kappa^3]^+$

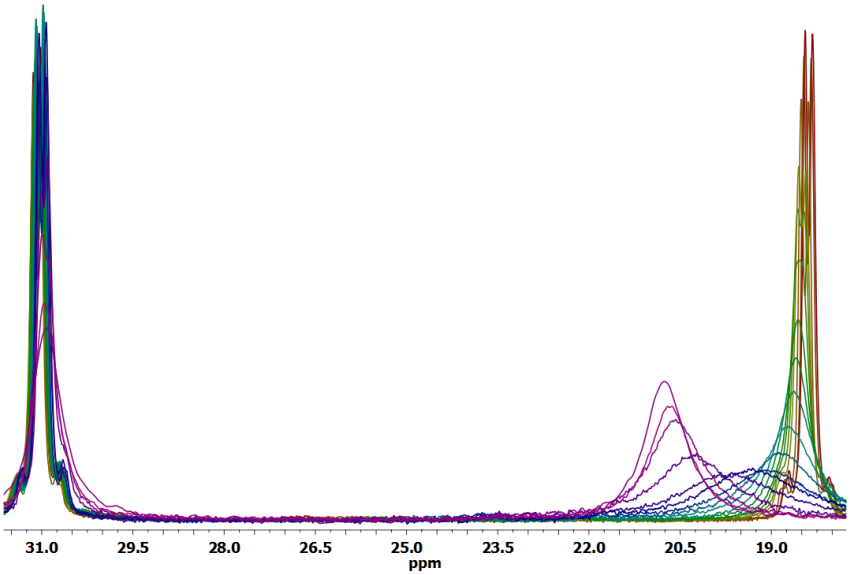

Variable temperature ^{31}P NMR spectra for **$3[\kappa^3]^+$** from 241K (red) to 354K (purple). The selected region depicts the bppm ligand (left) and the P_2N_2 ligand (right).

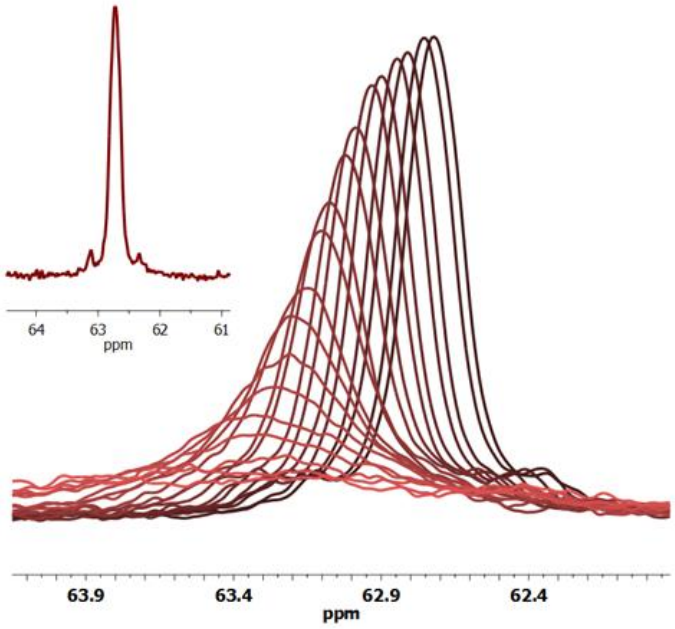

Variable temperature ^{31}P NMR spectra of a solution of **$3[\kappa^3]^+$** from 226K (maroon) to 270K (red). The selected region depicts the P_2N_2 ligand of the minor isomer. The inset depicts the 226K spectrum alone, highlighting the observable second-order coupling multiplet components.

Figure S3. Eyring (top) and van't Hoff (bottom) plots for the interconversion of 3[κ^3] and 3[$\kappa^2_{agostic}$].

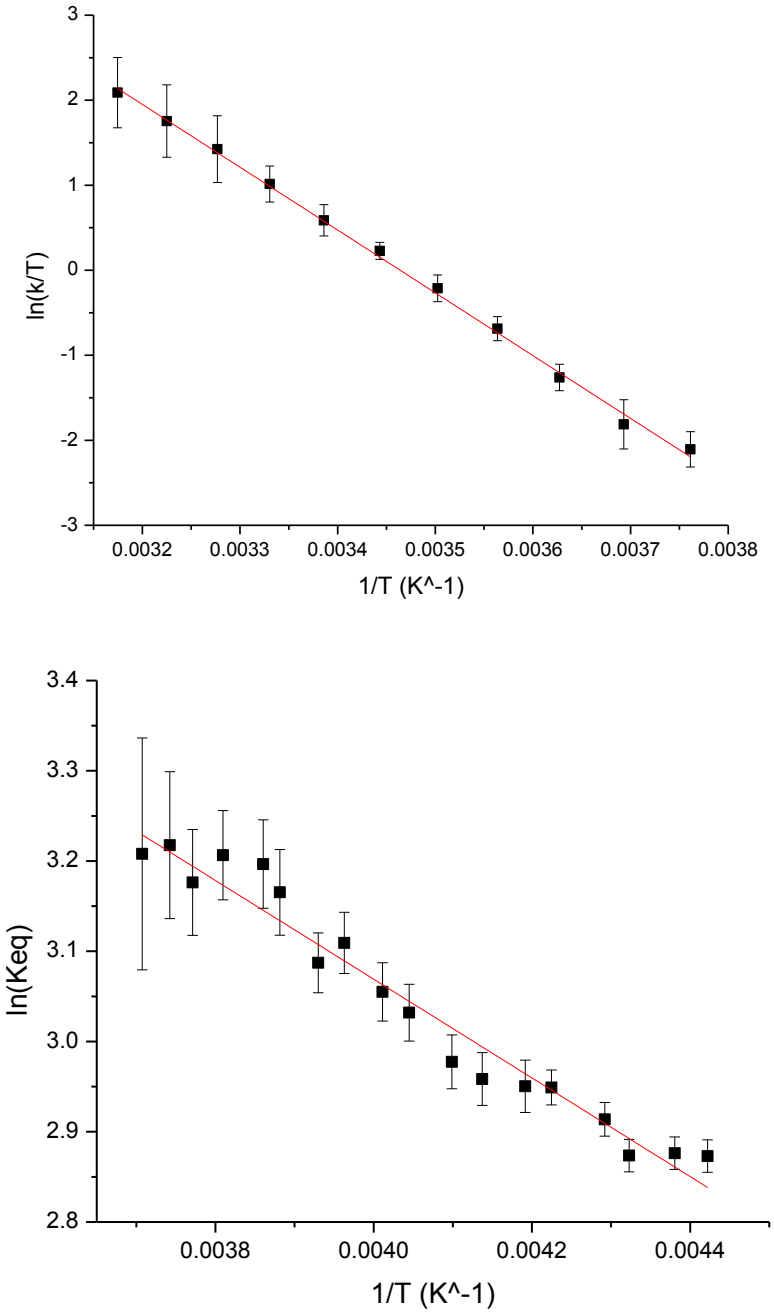

Figure S4. $^{1}H\{^{31}P\}$ EXSY Spectrum of 3[κ^3] in CD_2Cl_2 at –15 °C

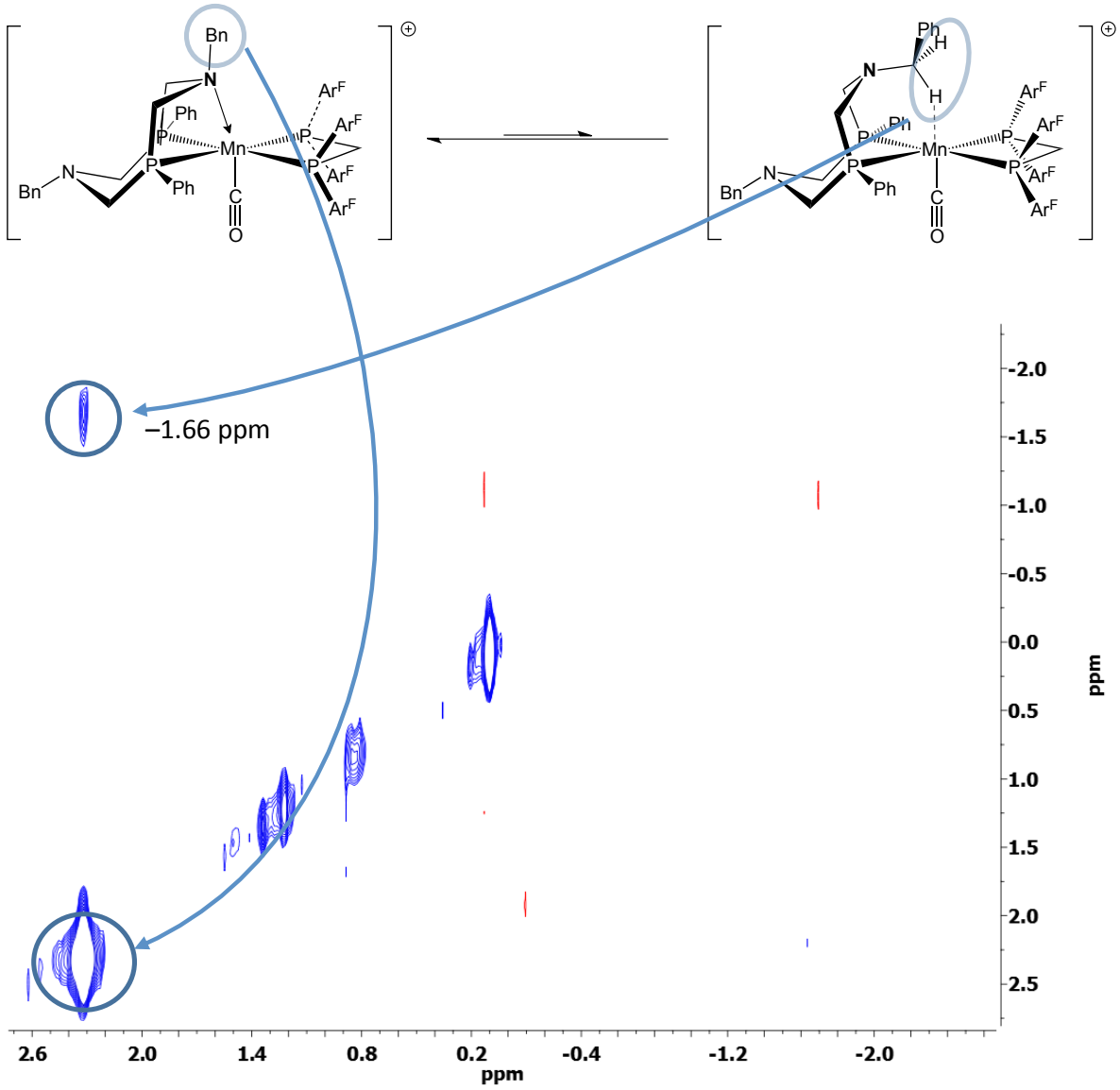

Acquired with a 200 ms mixing time; crosspeaks arising from the benzyl CH_2 protons of the κ^3 and $\kappa^3_{agostic}$ isomers have been indicated.

Figure S5. $^{31}P\{^{1}H\}$ EXSY Spectrum of 3[κ^3] in PhF at –15 °C

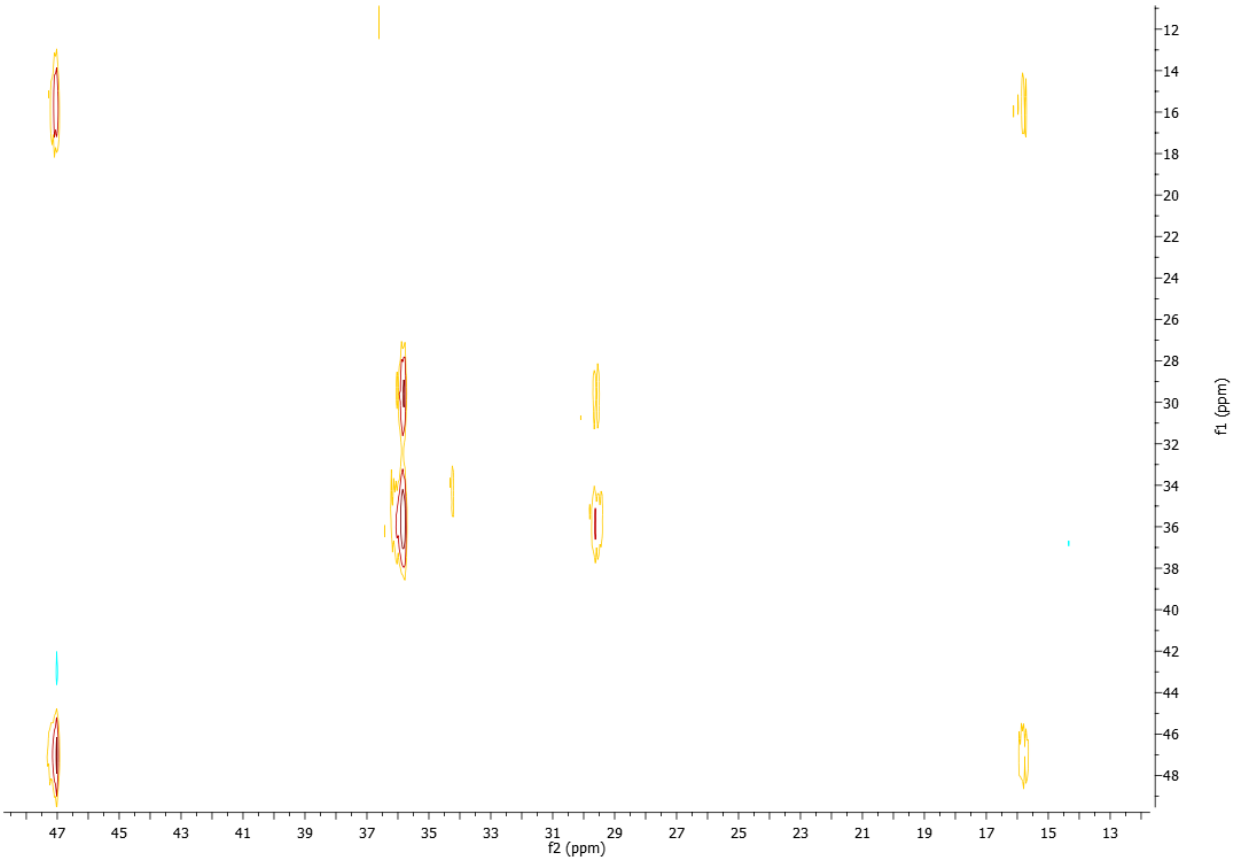

Figure S6. $^{31}P\{^{1}H\}$ Spectra of 4[κ²]/4[κ³] in PhF at –10 °C and 20 °C

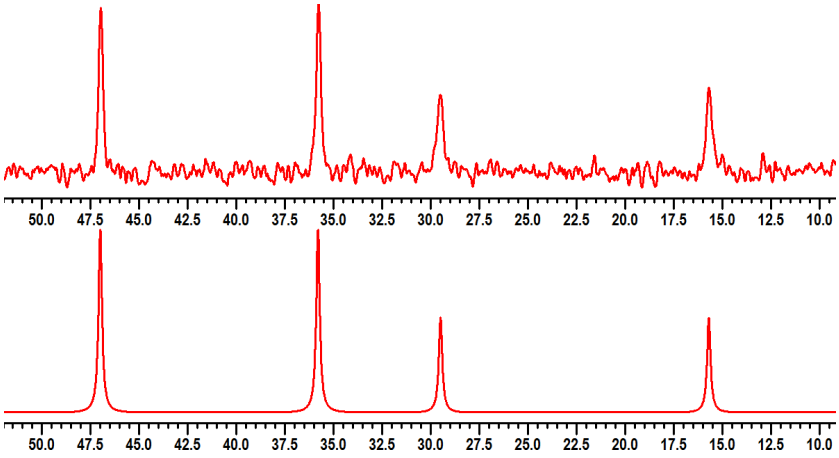

Experimental (top) and simulated (bottom) $^{31}P\{^{1}H\}$ spectra for **4[κ³]/4[κ²]** at –10 °C in PhF. The simulation assumed no exchange to obtain an estimate for the inherent linewidth (42 Hz). Both isomers are second-order spin systems (AA'BB'), but at this temperature the linewidth (either due to residual exchange effects or other issues) is sufficiently large that the coupling is not visible.

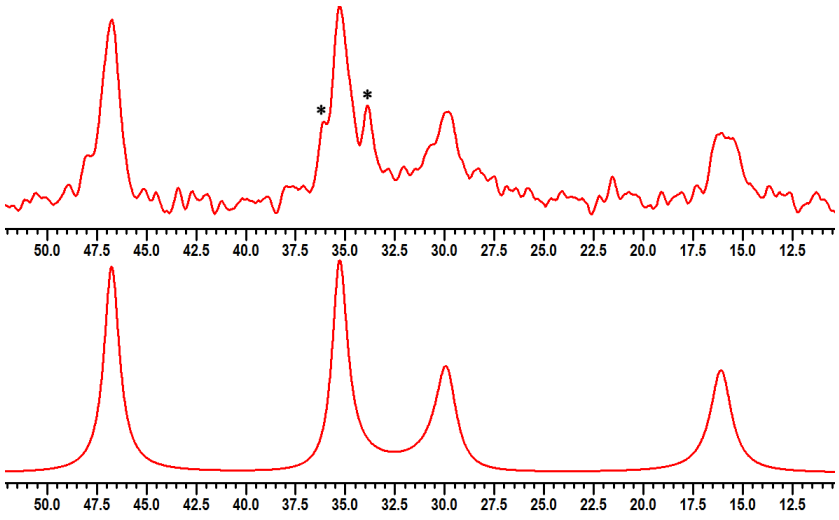

Experimental (top) and simulated (bottom) $^{31}P\{^{1}H\}$ spectra for $\mathbf{4[\kappa^2]^+/4[\kappa^3]^+}$ at 20 °C in PhF. The simulation, based on an inherent linewidth of 42 Hz, also takes into account a **4[κ²]⇋4[κ³]** exchange rate of 4.6×10^2 s^{-1}. Due to the low signal-to-noise in the spectrum, this is taken as a rough estimate only. The peaks marked with asterisks (*) denote signals from the impurity $\mathbf{4[CO]^+}$, small amounts of which invariably form during studies of $\mathbf{4[\kappa^2]^+}$.

Figure S7. $^{1}H\{^{31}P\}$ NMR Spectrum of 3-H/NH^{+} Isomers

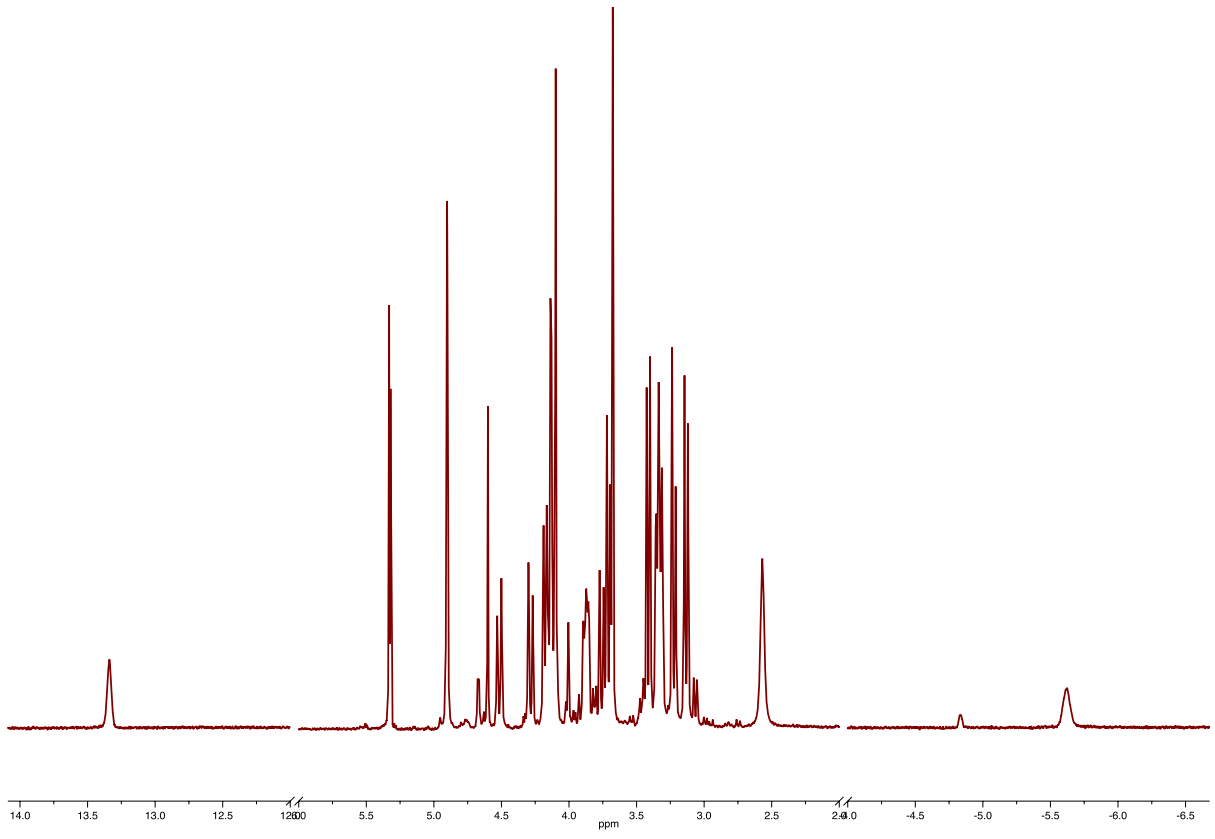

Figure S8. $^{31}P\{^{1}H\}$ NMR Spectrum of 3-H/NH^{+} Isomers

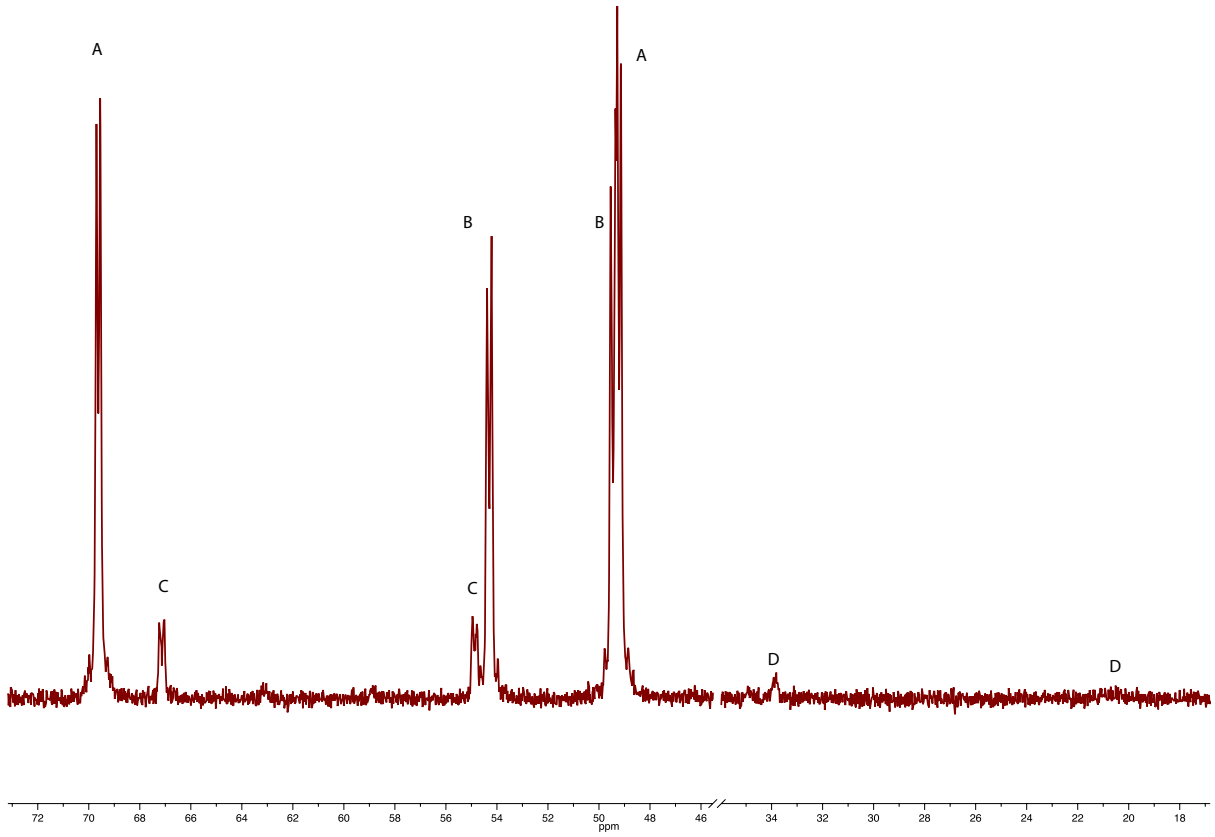

Assignment of species: A: ***syn,endo*-3-H/NH**; B: ***syn,exo*-3-H/NH**; C: ***anti,endo*-3-H/NH**; D: **3[κ^{3}]$^{+}$**

Figure S9. ^{15}N and $^{15}N\{^{1}H\}$ NMR Spectra of ^{15}N-Labelled 3-H/NH^{+} Isomers

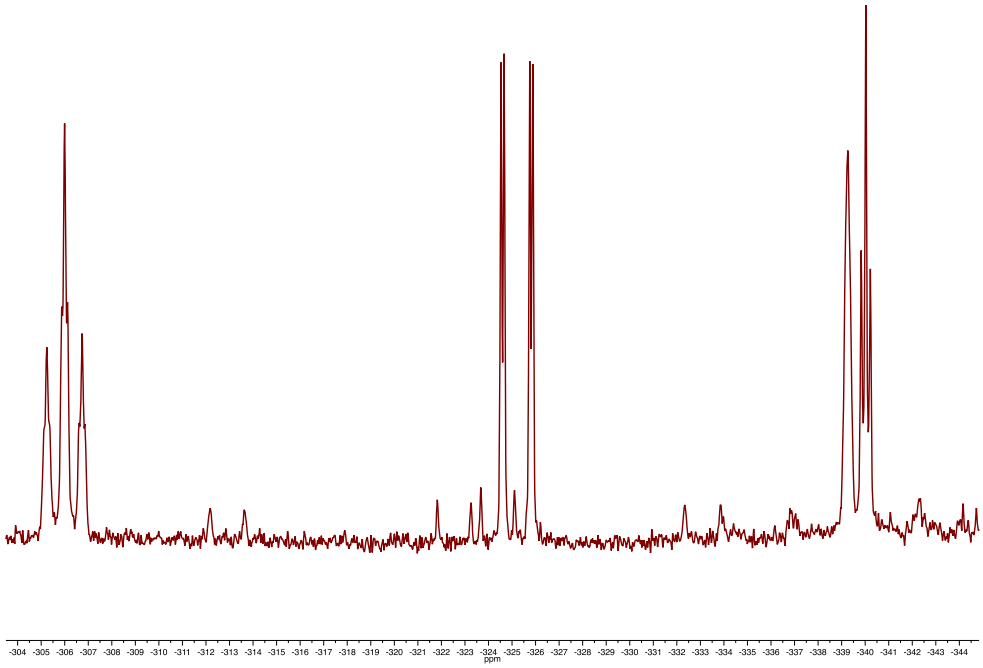

^{15}N NMR spectrum acquired at –47 ºC in CD_2Cl_2.

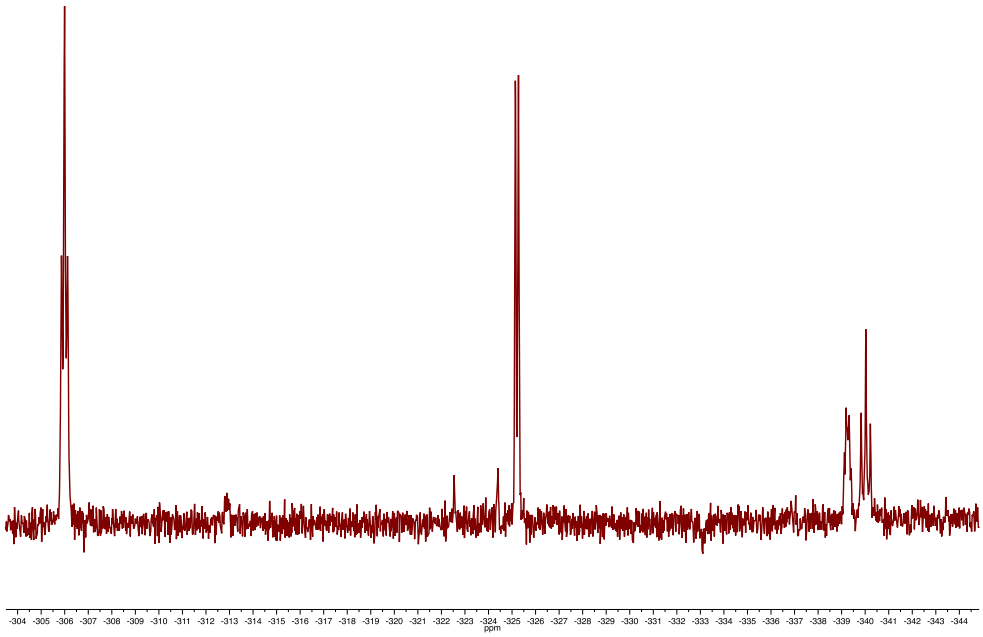

$^{15}N\{^{1}H\}$ NMR spectrum acquired at –47 ºC in CD_2Cl_2.

Figure S10. ^{1}H-^{15}N HSQCADTOXY Spectrum of ^{15}N-Labelled 3-H/NH^{+} Isomers

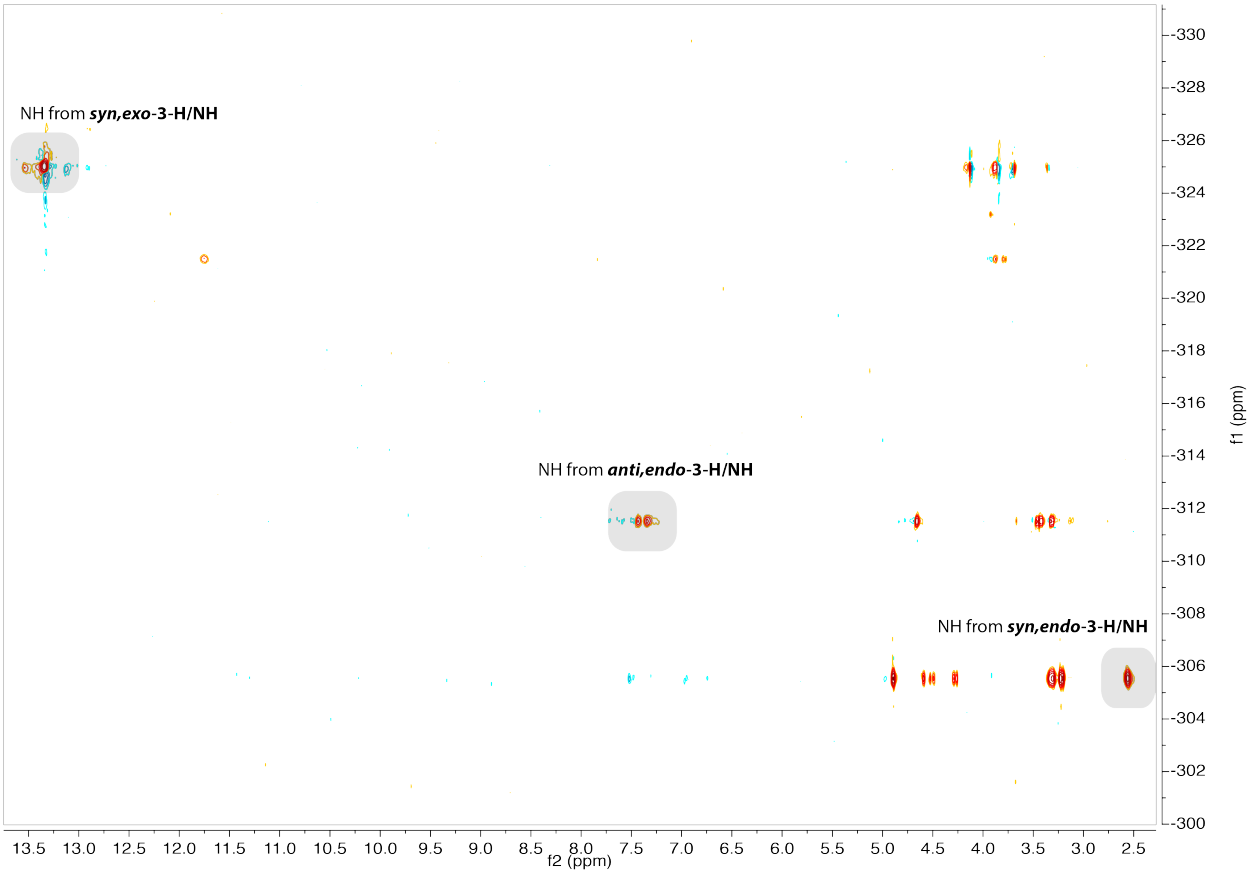

Figure S11. ^{2}H NMR Spectrum of 3-D/ND^{+} Isomers

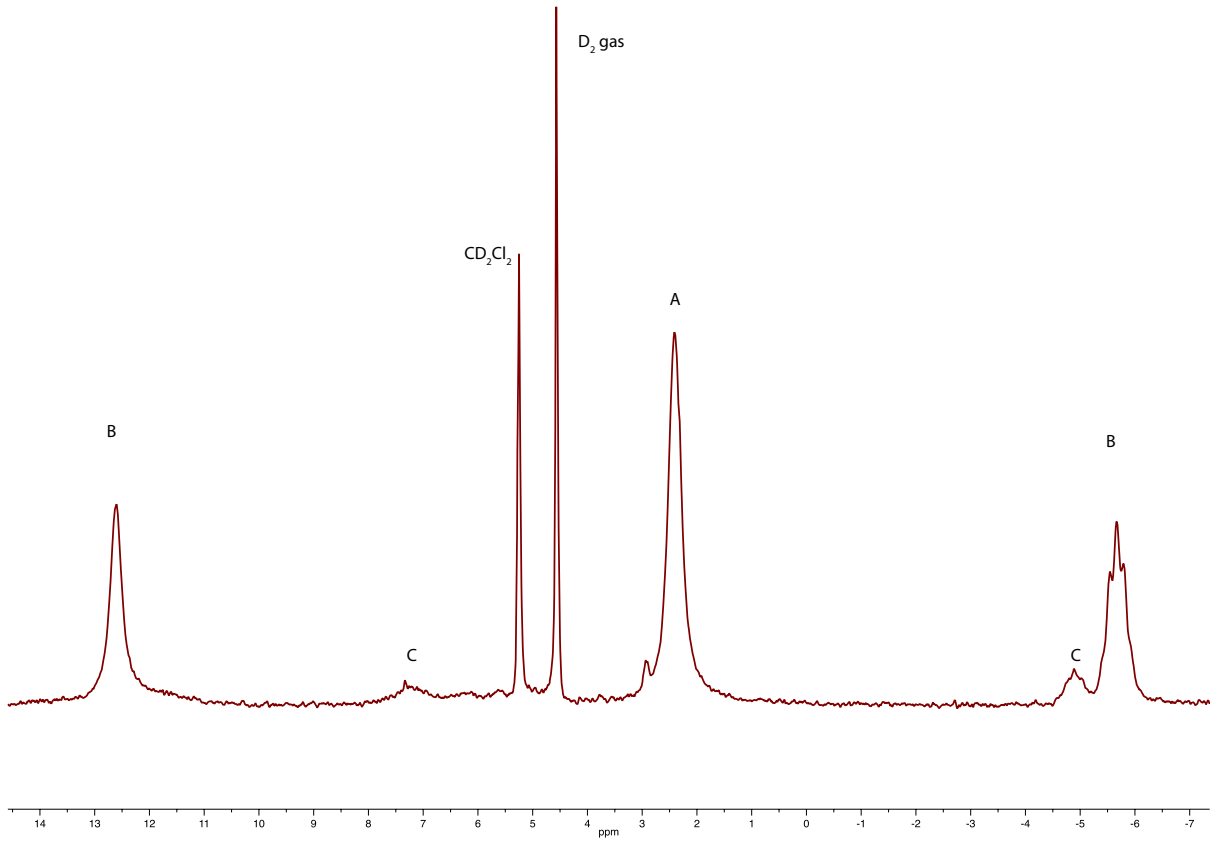

Assignment of species: A: ***syn,endo*-3-D/ND**; B: ***syn,exo*-3-D/ND**; C: ***anti,endo*-3-D/ND**

NMR Spectroscopic Assignment of 3-H/NH$^+$ Isomers

Since the crystal structures of the neutral ($P^{Ph}_2N^{Bn}_2$)Mn(H)(CO)(bppm) (see below) and the precursor ($P^{Ph}_2N^{Bn}_2$)Mn(Br)(CO)(bppm) both show chair-boat stereochemistries, it seems likely that the lowest energy stereoisomers of the protonated hydrides would involve either chair-boat or boat-chair conformations. Although alternative conformers with similar protonation topology are possible, NMR and computational studies on the related Ni(P_2N_2)$_2$ systems[4] indicate that ring-flips should be relatively facile and they are thus likely playing a dynamic role on the NMR timescale. For simplicity, the structures drawn in Figure 10 (main text) reflect the assumption of the lowest-energy conformer.

Based on the assignment of the 2.56 ppm ^{1}H NMR resonance as the rapidly equilibrating proton-hydride environment, we used TOCSY correlations to establish which P_2N_2 aliphatic (3.22 and 3.32 ppm) and benzyl protons (4.90 ppm) are *syn* to the hydride and, by elimination, those which are *anti* to the hydride (3.13 ppm, 3.41 ppm and 3.68 ppm, respectively). A ROESY crosspeak from the *anti* benzyl-CH_2 to one of the *syn* P_2N_2 CH_2 proton signals (3.32 ppm) established the inner- vs. outer-CH_2 signals, but this could not reliably be repeated for the other isomers, since the existence of similar ROESY and TOCSY crosspeaks meant that one effect could not reliably be extracted from the other. For the purposes of making stereochemical assignments, ROESY correlations were only considered when there was an absence of a correlation in the TOCSY spectra. The *syn* vs. *anti* bppm CH_2 protons for the three isomers were assigned via ROESY correlation to the *ortho*-CH of the bppm aryl groups and the hydride resonance. The *syn* vs. *anti* assignment of the P_2N_2 benzyl groups of *anti,endo*-**3-H,NH$^+$** isomer were made by the fortuitous observation of chemical exchange with the corresponding signals of the *syn,endo* isomer, presumably via the neutral hydride. The various correlations used to assign the remaining signals are summarized in Figure S12.

The stereochemical assignment of *syn,exo*-**3-H,NH$^+$** isomer requires more explanation. The ^{1}H NMR spectrum of the ^{15}N-labeled isomer manifests as a doublet at room temperature (J_{NH} = 55 Hz) and the two peaks of the doublet are relatively broad ($\nu_{½}$ = 22 Hz). At low temperature (223K) the doublet is slightly wider (J_{NH} = 63 Hz) but the doublet components retain the same degree of breadth. The ^{1}H,^{15}N-HSQCAD spectrum shows a strong correlation of the proton signal at 13.33 ppm with an ^{15}N nucleus at –325.2 ppm. When the same experiment is performed with the J-selector set to 12 Hz, an additional correlation can be observed correlating the 13.33 ppm proton with another ^{15}N nucleus at –337.0 ppm. This establishes that this proton is in some way correlated to two ^{15}N environments, indicating the general stereochemical arrangement assigned in Figure X. The ^{15}N NMR signals for these two nitrogen nuclei strengthen the argument for the given structure. The ^{15}N NMR resonance at –325.2 ppm manifests as a doublet of doublets (J = 7 Hz, 55 Hz) that collapses to a doublet (J = 7 Hz) upon broadband ^{1}H decoupling. The 7 Hz doublet is most telling – although consistent in magnitude to J_{NP} coupling, coupling to the two ^{31}P nuclei would result in a triplet, thus the most likely cause is J_{NN} coupling to the second ^{15}N nucleus via an N-H-N bridge. Of course, the fact that the 13.33 ppm proton signal is a clear doublet means that ^{15}N coupling is essentially dominated by a single ^{15}N nucleus. The most straightforward way to rationalize these results is to propose the series of structures (depicted below) which shows three possible structures with varying P_2N_2 stereochemistry while retaining *exo* protonation.

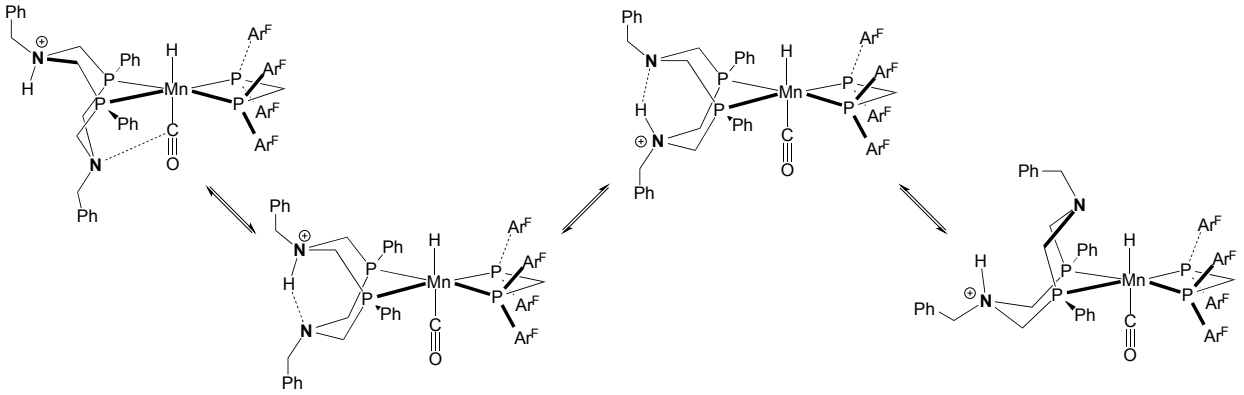

The N→CO interaction depicted by the dashed line in the first structure is invoked based on previous studies of $(P_2N_2)_2Ni(CO)$, where both the uncharacteristic affinity of the Ni complex for CO and close N-C_{CO} contacts were rationalized by a moderate N→CO interaction.[5] With the model presented in the above figure, the dynamics of *exo* protonation are dominated by the first and second structures, leading to an average where the proton is mostly interacting with the *syn* nitrogen.

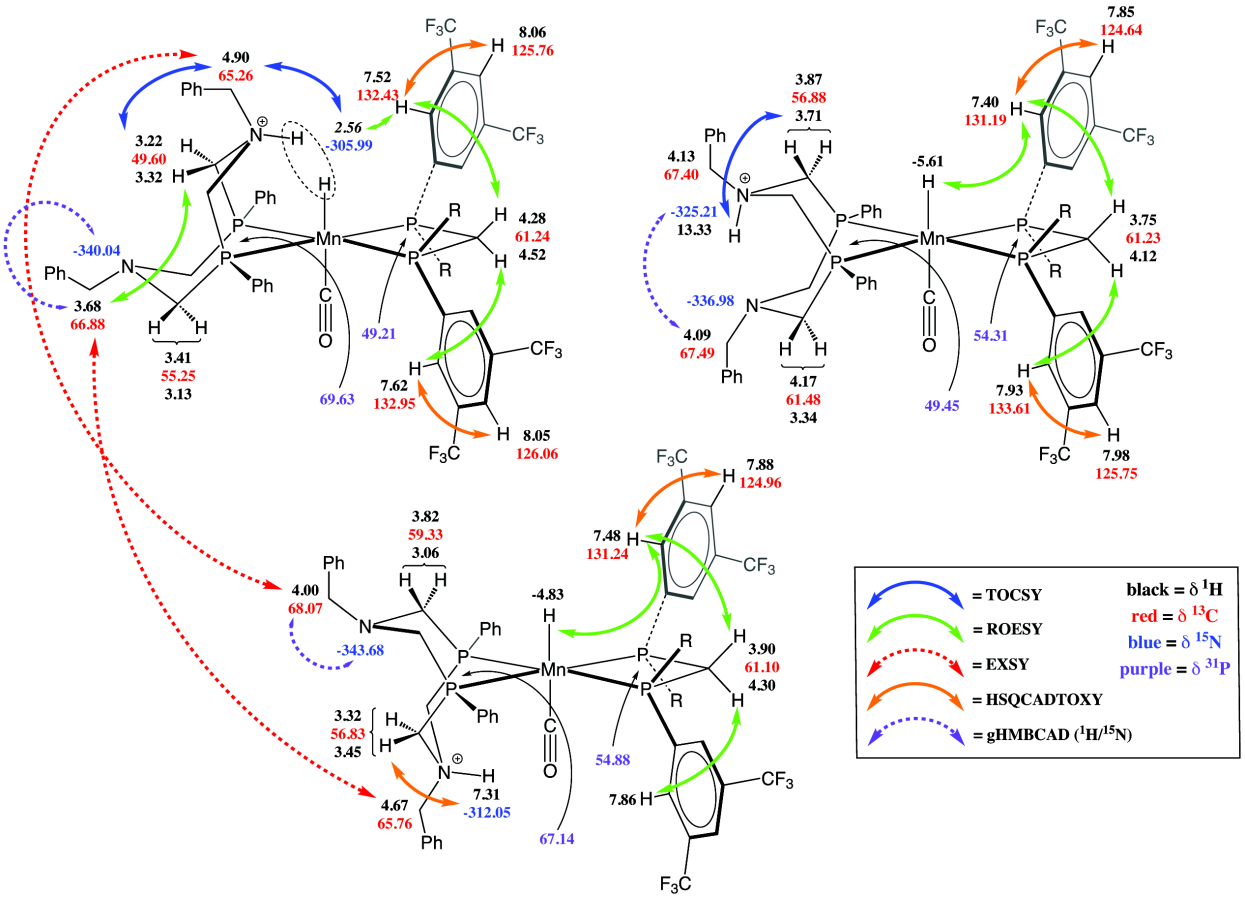

Figure S12. Summary of NMR Spectroscopic Assignments of 3-H,NH$^+$ Isomers

The stereochemistry of the *syn,exo* isomer of **3-H/NH** is shown with chair/chair stereochemistry (and concomitant N-H•••N interaction) to highlight the likely pathway for the long-range coupling observed in the ^{1}H/^{15}N-gHMBCAD experiment. This interaction is likely dynamic, as discussed above (**NMR Spectroscopic Assignment of 3-H/NH$^+$ Isomers**).

Details of fitting procedure used to simulate portions of the ^{1}H NMR spectra of *syn*-4-H,NH$^+$

Selected portions of the ^{1}H NMR spectra of *syn*-**4-H,NH**$^+$ were simulated to extract rate constants for proton/hydride exchange. This procedure was complicated by a significant temperature dependence in some of the chemical shifts, notably the peak for the NH proton (as observed at –52 ºC through –31 ºC) and the average NH/MnH peak (as observed at 41 ºC through 62 ºC). Although there is a small (but observable) temperature dependence in the MnH signal, the temperature dependence of the average NH/MnH peak is likely to be primarily due to the NH chemical shift.

The temperature dependence of the chemical shifts arises from two possible effects, both of which are likely operative. The first is due to the dynamic equilibrium between isomeric complexes en route to the transition state for proton/hydride exchange. The proton/hydride exchange encompasses at least two microscopic steps; boat-to-chair isomerization followed by proton/hydride exchange via the Mn(η^2-H_2) complex.

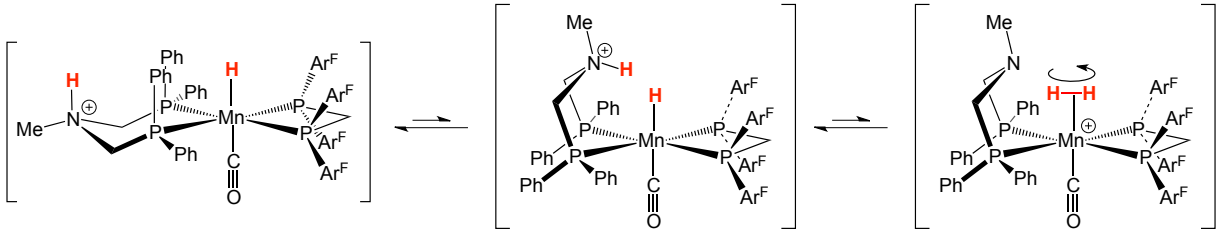

It is currently not known which step is rate-limiting since the energetic position of the boat form relative to the chair form is unknown. In either case, the observed exchange ultimately involves three species, the chair and boat forms of *syn,endo*-**4-H,NH**$^+$ and **4-(η^2-H_2)**$^+$, and an equilibrium between the two lower energy structures. This equilibrium, being temperature dependent (to whatever degree), would naturally influence the weighted average chemical shift of the observed

protons. The second mechanism for a solvent dependence would be due to changing interactions with the solvent environment and/or the non-coordinating anion $B(C_6F_5)_4^-$. Although interactions with non-polar fluorobenzene would likely not contribute much to the temperature dependent chemical shifts of ligand C-H protons, the NH proton may be strongly influenced by changing solvent interactions. It is possible that NH···FPh (cation/solvent) and/or NH···F-$C_6F_4B(C_6F_5)_3$ (cation/anion) interactions remain significant in solution; indeed, the solid-state structure of [***syn*-4-H,NH$^+$**][$B(C_6F_5)_4$]•d_5-PhBr reveals a NH···Br interaction (d(NH···Br) = 2.834 Å) with co-crystallized solvent. The temperature dependence of the NH chemical shift presented a problem for simulation, as the NH/MnH peak separation ($\Delta\delta$, ppm) is a key parameter in calculating the rate of chemical exchange. The chemical shifts of three ^{1}H NMR resonances for ligand protons (specifically the signals for the NC*H*$_3$ protons, one of the bppm C*H*H protons, and one of the PNP C*H*H protons) were plotted against the observed temperature range and were found to fit a quadratic relationship with temperature (Figure S14). The MnH resonances at low temperature were also fit to a quadratic function, revealing a relatively small temperature dependence ($\Delta\delta$ ~ 0.3 ppm from –51 ºC to 62 ºC), which was used in combination with the measured value for the average NH/MnH peak to back-calculate the NH chemical shift at 41 ºC through 62 ºC. These six values were also fit to a quadratic function to interpolate values for the NH chemical shift at intermediate temperatures (Figure S15).

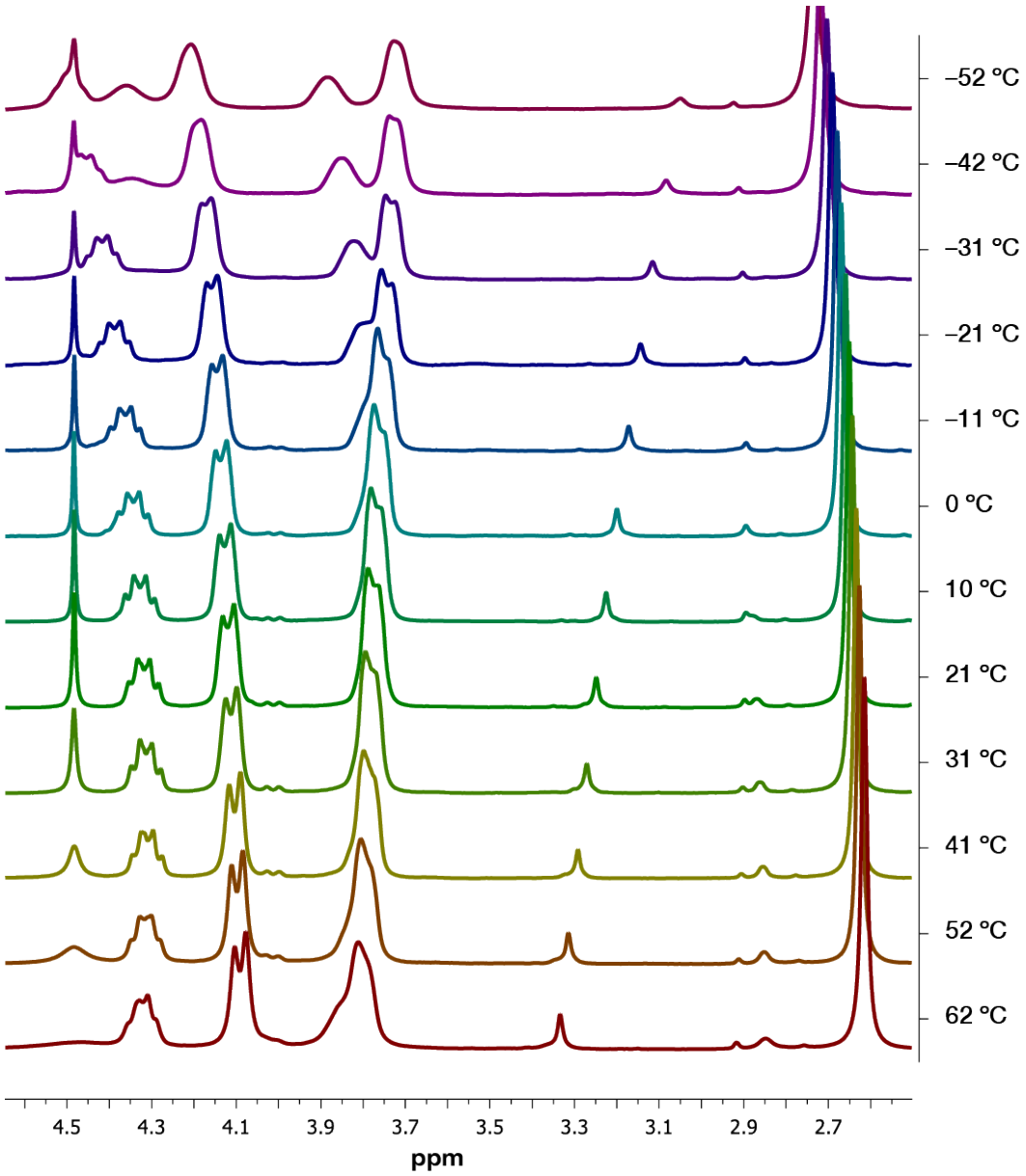

Figure S13. Variable temperature ^{1}H NMR spectra for ligand region of *syn*-4-H,NH

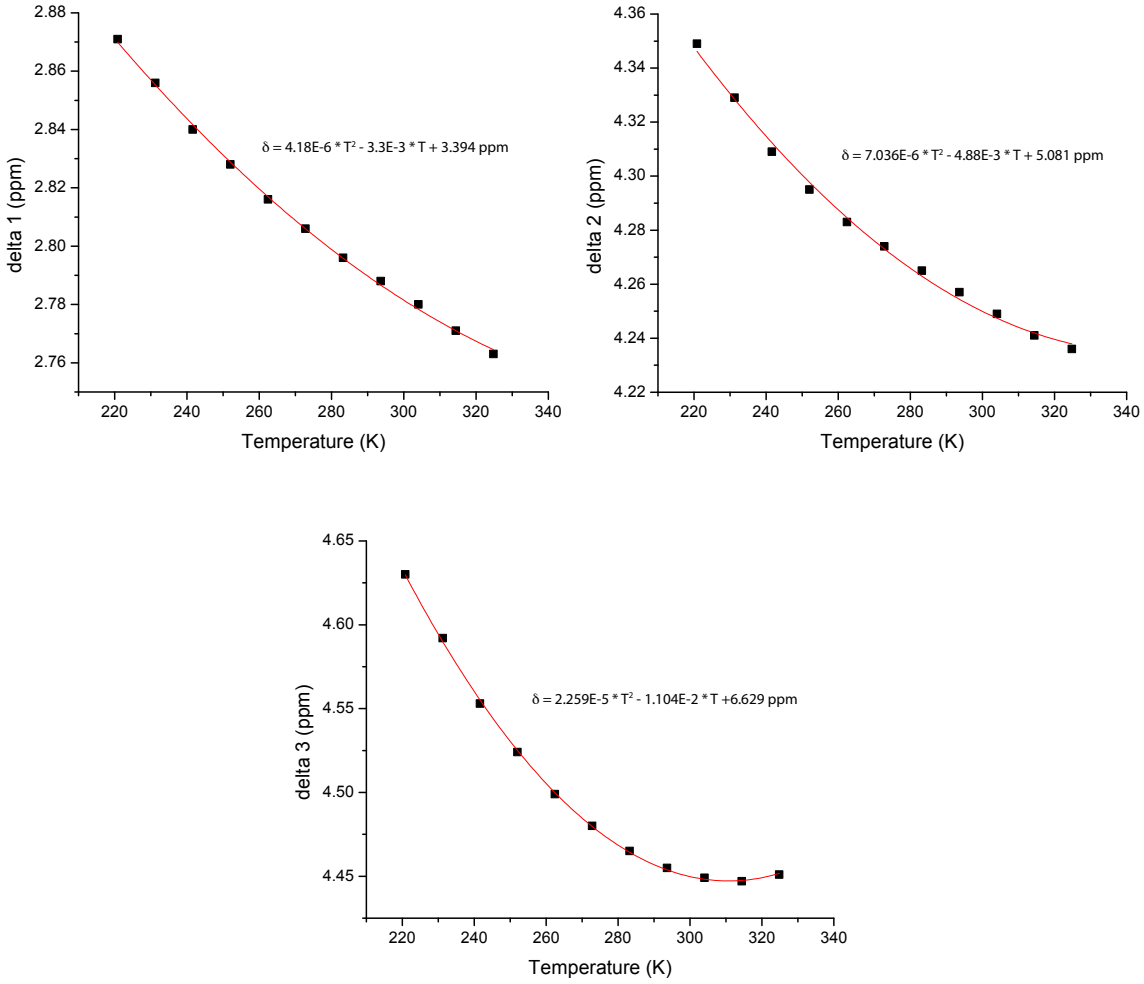

Figure S14. Temperature dependencies of ^{1}H chemical shifts for selected ligand protons

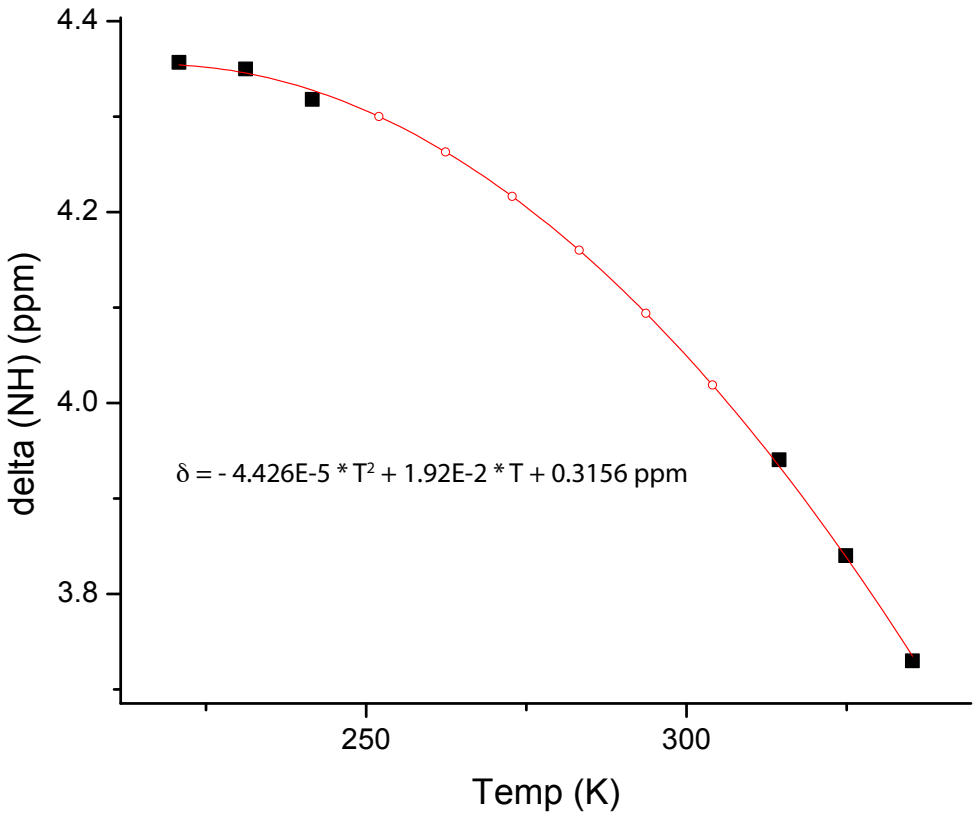

Figure S15. Temperature dependence of ^{1}H chemical shifts for the NH proton in 4-H,NH.

The polynomial fit to the experimental data (black squares) was used to interpolate the NH chemical shifts (open red circles) used in the spectral simulations.

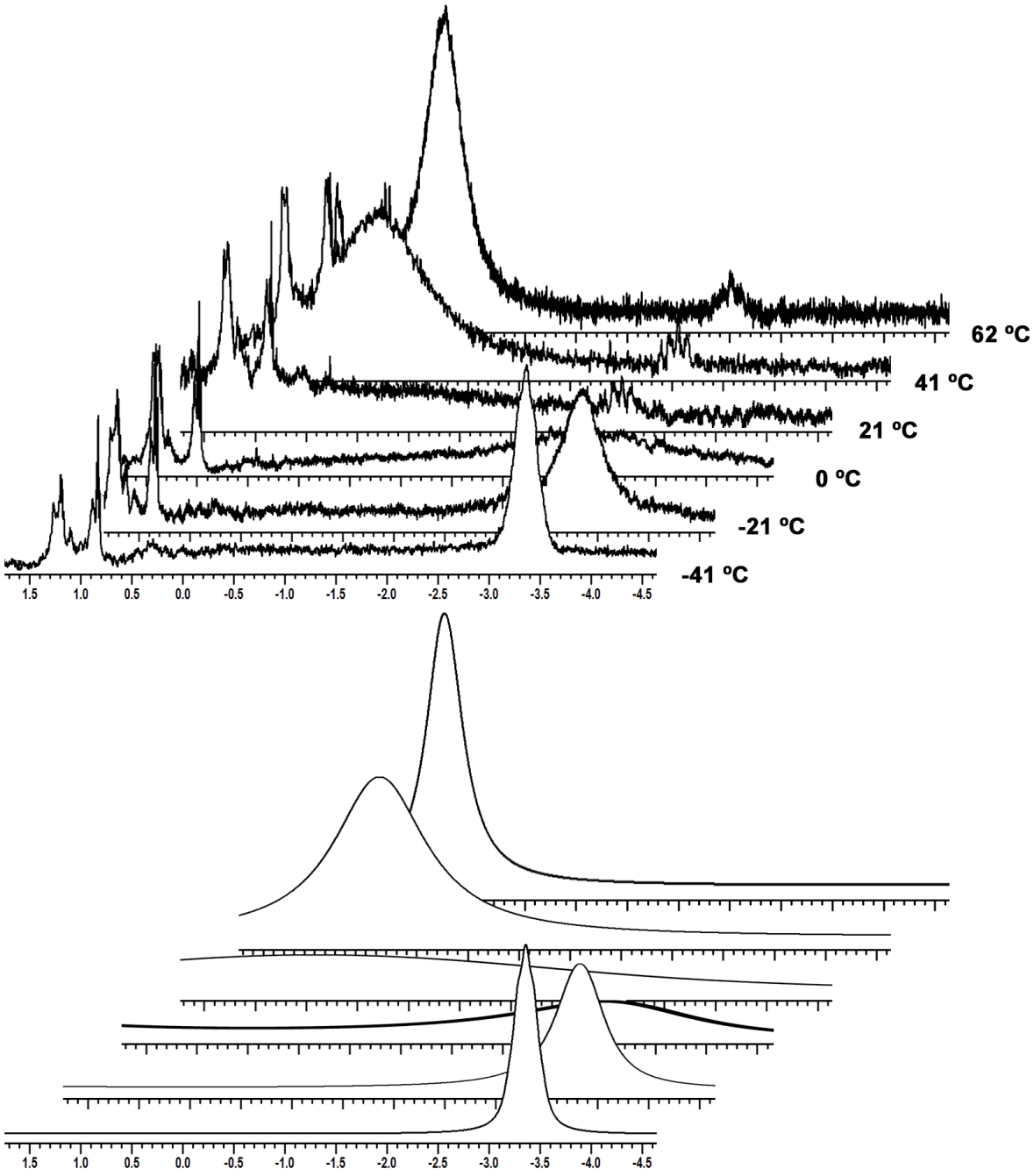

Figure S16. Experimental and Simulated ^{1}H NMR spectra for *syn*-4-H,NH

Selected simulations from –41 ºC to 62 ºC; only the MnH/NH average (high T) and MnH (low T) regions are shown. The sharp peaks between 0.8–1.4 ppm are from pentane and the multiplet at –2.5 ppm (visible at higher temperatures) is assigned to the *anti*-**4-H,NH** isomer.

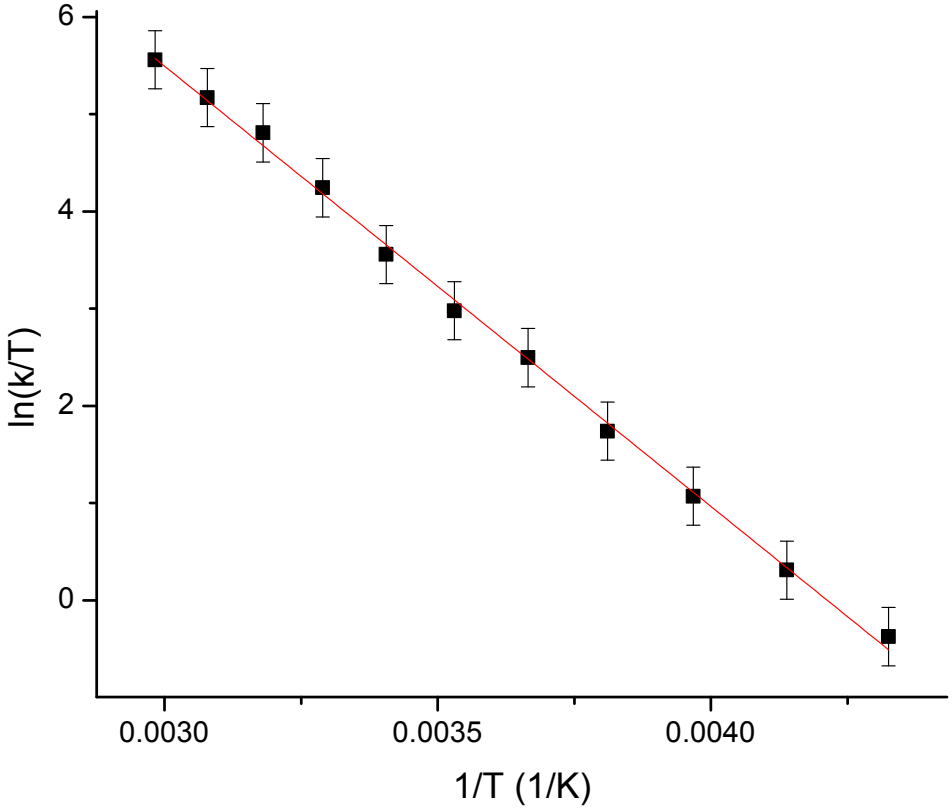

Figure S17. Eyring Plot for Rates of Proton/Hydride Exchange in *syn*-4-H,NH

Figure S18. Space-filling Models of $2[\kappa^3]^+$ and $3[\kappa^3]^+$

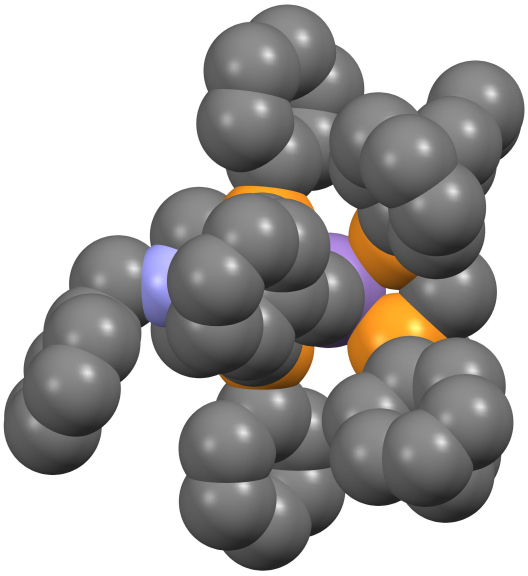

Space-filling model of **$2[\kappa^3]^+$** viewed down the Mn-CO axis.

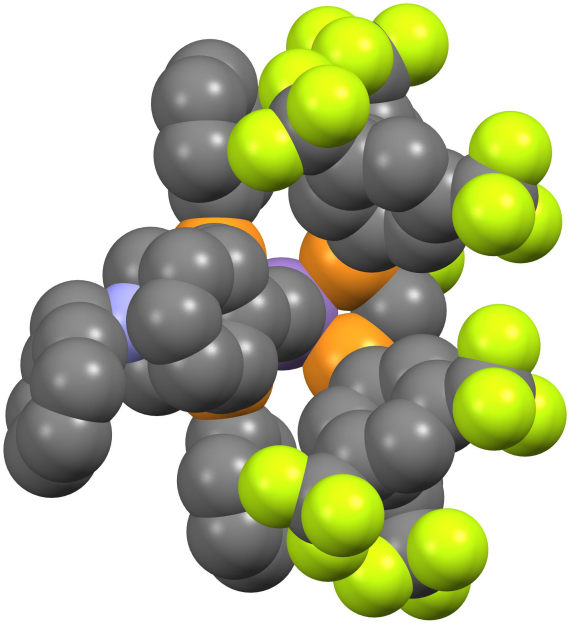

Space-filling model of **$3[\kappa^3]^+$** viewed down the Mn-CO axis.

Figure S19. Computed Structures of $1[\kappa^3]^+$, $4[\kappa^3]^+$, and $5[\kappa^3]^+$
Hydrogen atoms not shown.

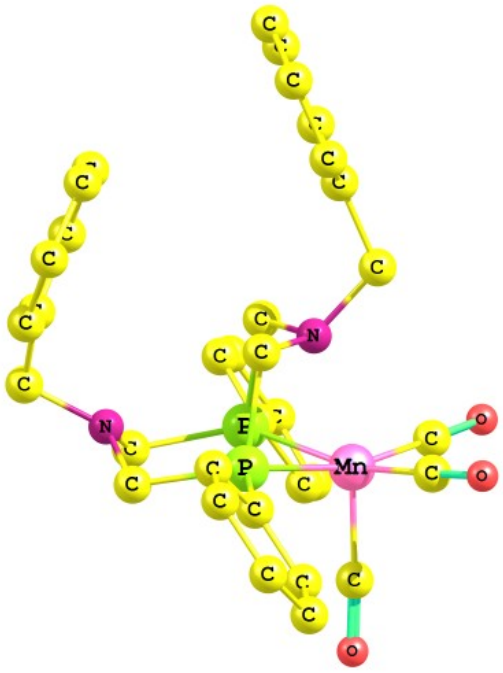

$1[\kappa^3]^+$

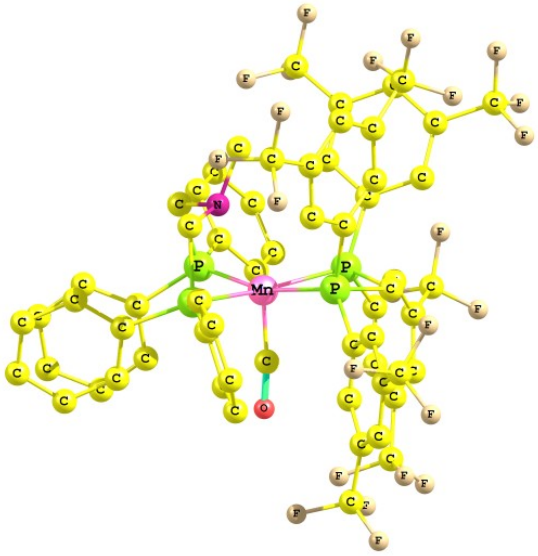

$4[\kappa^3]^+$

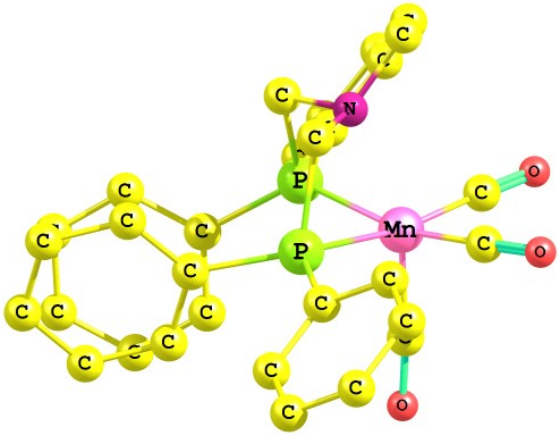

$5[\kappa^3]^+$

Figure S20. Molecular Structure of $(P^{Ph}N^{Me}P^{Ph})Mn(CO)_2(bppm)]^+[B(C_6F_5)_4]^-$ (4[CO]$^+$)

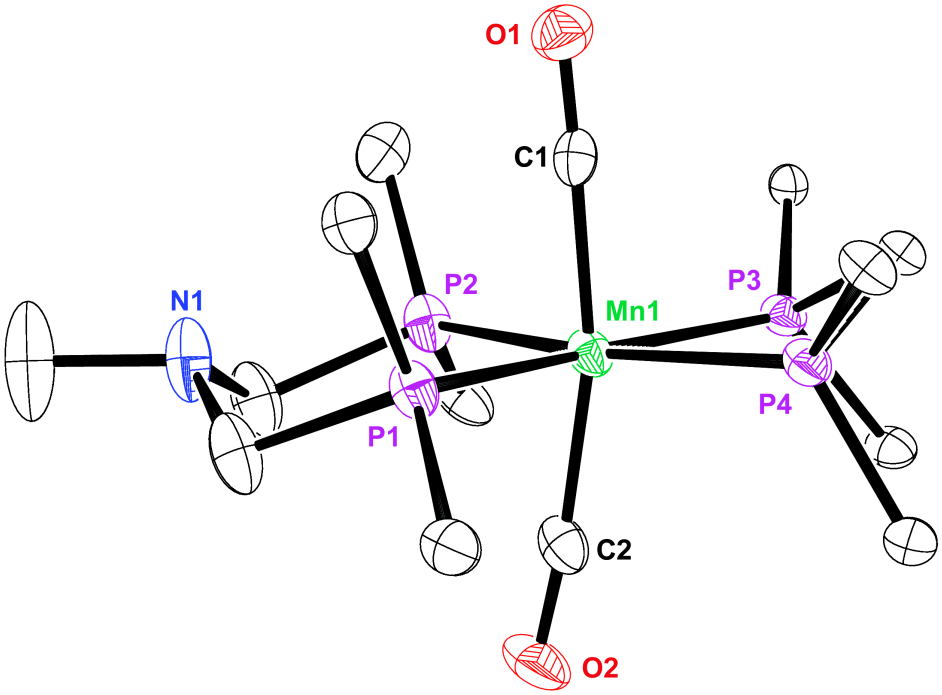

Solid-state molecular structures of $[(P^{Ph}N^{Me}P^{Ph})Mn(CO)_2(bppm)]^+[B(C_6F_5)_4]^-$ (**4[CO]$^+$[B(C$_6$F$_5$)$_4$]$^-$**, at –173 °C). Substituents on the P have been truncated, and hydrogen atoms and co-crystallized PhF have been omitted for clarity.

Donor/Acceptor NBO Calculation Output for $3[\kappa^3_{agostic}]^+$

```
Second Order Perturbation Theory Analysis of Fock Matrix in NBO Basis

Threshold for printing:   0.50 kcal/mol

                                                                    E(2)  E(j)-E(i) F(i,j)
        Donor NBO (i)                    Acceptor NBO (j)          kcal/mol   a.u.    a.u.
 ================================================================================================

73. BD (   1) C  28 - H 113        /297. LP*(   4)Mn   1                64.72    0.86    0.210
73. BD (   1) C  28 - H 113       /373. RY*(   1)Mn   1                  1.20    1.41    0.039
73. BD (   1) C  28 - H 113       /375. RY*(   3)Mn   1                  0.65    1.49    0.029
73. BD (   1) C  28 - H 113       /388. RY*(  16)Mn   1                  0.70    2.19    0.037
73. BD (   1) C  28 - H 113       /391. RY*(  19)Mn   1                  2.34    3.64    0.087
73. BD (   1) C  28 - H 113       /392. RY*(  20)Mn   1                  2.35   38.82    0.283
73. BD (   1) C  28 - H 113       /405. RY*(   3) P   2                  1.00    2.05    0.042
73. BD (   1) C  28 - H 113       /414. RY*(  12) P   2                  0.55    3.11    0.039
73. BD (   1) C  28 - H 113       /422. RY*(   3) P   3                  0.99    1.99    0.042
73. BD (   1) C  28 - H 113       /439. RY*(   3) P   4                  0.65    1.68    0.031
73. BD (   1) C  28 - H 113       /444. RY*(   8) P   4                  0.52    2.57    0.034
73. BD (   1) C  28 - H 113       /456. RY*(   3) P   5                  1.11    1.94    0.044
73. BD (   1) C  28 - H 113       /480. RY*(   1) N   7                  0.96    1.57    0.036
73. BD (   1) C  28 - H 113       /489. RY*(   1) C   8                  0.68    1.58    0.031
73. BD (   1) C  28 - H 113       /492. RY*(   4) C   8                  0.81    3.70    0.051
73. BD (   1) C  28 - H 113       /652. RY*(   2) C  26                  1.18    1.70    0.042
73. BD (   1) C  28 - H 113       /***. BD*(   1)Mn   1 - C   8          6.58    1.26    0.084
73. BD (   1) C  28 - H 113       /***. BD*(   1) P   3 - C  21          0.55    0.79    0.019
73. BD (   1) C  28 - H 113       /***. BD*(   2) C  26 - C  58          1.00    0.64    0.024
73. BD (   1) C  28 - H 113       /***. BD*(   1) C  26 - C  78          2.70    1.22    0.053
73. BD (   1) C  28 - H 113       /***. BD*(   1) C  28 - H 113          2.54    1.02    0.047

298. LP (   1) N   6              /589. RY*(   2) C  19                  1.70    1.68    0.049
298. LP (   1) N   6              /592. RY*(   5) C  19                  0.53    2.15    0.031
298. LP (   1) N   6              /607. RY*(   2) C  21                  1.61    1.73    0.049
298. LP (   1) N   6              /913. RY*(   2) C  55                  1.03    1.51    0.036
298. LP (   1) N   6              /914. RY*(   3) C  55                  0.76    1.56    0.032
298. LP (   1) N   6              /***. BD*(   1) P   3 - C  21          1.52    0.60    0.027
298. LP (   1) N   6              /***. BD*(   1) P   4 - C  19          1.53    0.61    0.028
298. LP (   1) N   6              /***. BD*(   1) C  15 - H 102          1.01    0.90    0.028
298. LP (   1) N   6              /***. BD*(   1) C  19 - H 103          9.08    0.86    0.081
298. LP (   1) N   6              /***. BD*(   1) C  21 - H 106          9.85    0.86    0.084
298. LP (   1) N   6              /***. BD*(   1) C  21 - H 107          0.56    0.88    0.020
298. LP (   1) N   6              /***. BD*(   1) C  37 - C  55          1.66    0.88    0.035
298. LP (   1) N   6              /***. BD*(   1) C  55 - H 129          7.79    0.88    0.076
298. LP (   1) N   6              /***. BD*(   1) C  55 - H 130          0.63    0.90    0.022

299. LP (   1) N   7              /544. RY*(   2) C  14                  1.63    1.70    0.050
299. LP (   1) N   7              /553. RY*(   2) C  15                  1.52    1.67    0.047
299. LP (   1) N   7              /670. RY*(   2) C  28                  1.03    1.53    0.037
299. LP (   1) N   7              /672. RY*(   4) C  28                  0.94    2.21    0.043
299. LP (   1) N   7              /***. BD*(   1) P   3 - C  14         16.56    0.56    0.088
299. LP (   1) N   7              /***. BD*(   1) P   4 - C  15         16.58    0.56    0.089
299. LP (   1) N   7              /***. BD*(   1) C  14 - H  99          1.62    0.87    0.035
299. LP (   1) N   7              /***. BD*(   1) C  14 - H 100          1.55    0.87    0.035
299. LP (   1) N   7              /***. BD*(   1) C  15 - H 101          2.14    0.87    0.041
299. LP (   1) N   7              /***. BD*(   1) C  15 - H 102          1.10    0.88    0.029
299. LP (   1) N   7              /***. BD*(   1) C  26 - C  28          2.79    0.85    0.045
299. LP (   1) N   7              /***. BD*(   1) C  28 - H 113         12.71    0.82
0.095
```

NBO donor-acceptor calculations support both the proposed agostic interaction (C28-H113/Mn, in blue) and the N(sp^3)→C-H(σ*) hyperconjugation interaction (N7/C28-H113, in red). The results for the non-interacting pendant amine of the P_2N_2 ligand (N6) are shown for comparison.

X-ray Crystallography

Crystals selected for diffraction studies were immersed in Paratone-N oil, placed on a Nylon loop (MiTiGen MicroMounts), and transferred to a precooled cold stream of N_2. A Bruker KAPPA APEX II CCD diffractometer with 0.71073 Å Mo Kα radiation was used for diffraction studies. The space groups were determined on the basis of systematic absences and intensity statistics. The structures were solved by direct methods and refined by full-matrix least squares on F^2. All nonhydrogen atoms were refined anisotropically unless otherwise stated. Hydrogen atoms were placed at idealized positions and refined using the riding model. Data collection and cell refinement were performed using Bruker APEX2 software (1). Data reductions and absorption corrections were performed using Bruker's SAINT (2) and SADABS (3) programs, respectively. Structural solutions and refinements were completed using SHELXS-97 and SHELXL-97 (or SHELXL-13) (4), respectively, as implemented in the OLEX2 (v. 1.2, 64-bit Win7) software package (5).

1 Bruker (2007), APEX2 Program for Data Reduction; Bruker AXS.: Madison, WI.

2 Bruker (2007), SAINT Program for Data Reduction; Bruker AXS.: Madison, WI.

3 Sheldrick, G. SADABS Program for Absorption Correction of Area Detector Frames; University of Göttingen, Germany.

4 Sheldrick, G. A short history of SHELX. *Acta Crystallogr., Sect. A* **64**, 112-122 (2008).

5 Dolomanov, O.V.; Bourhis, L. J.; Gildea, R. J.; Howard, J. A. K.; Puschmann, H. OLEX2: a complete structure solution, refinement and analysis program. *J. Appl. Cryst.* **42**, 339-341 (2009).

Computational Methods

Calculations were performed with the Gaussian09 software package.[6] The dispersion-corrected functional ωB97XD[7] was used in conjunction with the 6-31G* basis-set for H, C, N, O and F atoms, 6-311G(d,p) for P atoms, and the Stuttgart basis set with effective core potential (ECP) for Mn.[8] Frequency calculations were performed on minimized structures to confirm the absence of imaginary frequencies. Single point calculations on the minimized structures of in a CH_2Cl_2 solvation model (C-PCM, Bondi radii) were performed on **3**$[\kappa^3]^+$, **3**$[\kappa^3_{agostic}]^+$, and **3**$[\kappa^2]^+$ to obtain approximate values for the solvation free energies.

XYZ-Coordinates for Computed Structures

1[κ³]⁺:

N	-0.043634000	-0.022334000	2.514207000
H	-0.833135000	-5.048306000	-3.339668000
Mn	1.197791000	1.454638000	-0.912247000
C	0.305849000	2.246051000	-2.296579000
P	1.997692000	0.021801000	0.731251000
P	-0.696492000	1.581051000	0.406045000
C	2.552822000	0.943071000	-2.028866000
N	0.102777000	-0.454918000	-1.023765000
C	2.017888000	2.987752000	-0.374755000
O	2.522533000	3.942681000	0.014492000
C	0.970682000	-1.260674000	-0.117954000
H	1.636253000	-1.872628000	-0.731682000
H	0.393490000	-1.908681000	0.547717000
C	-1.170746000	-0.021600000	-0.377649000
H	-1.605594000	-0.783069000	0.275178000
H	-1.890047000	0.207590000	-1.167551000
C	-2.067415000	2.740840000	0.182665000
C	3.707607000	-0.566357000	0.822754000
C	-0.668268000	1.248670000	2.232653000
H	-0.177650000	2.094679000	2.742466000
H	-1.708421000	1.228999000	2.565393000
C	1.396944000	-0.019645000	2.496478000
H	1.773724000	-0.946550000	2.939921000
H	1.854412000	0.818164000	3.050090000
C	-1.018329000	-2.380009000	-2.206929000
C	-1.811491000	4.049459000	-0.234563000
H	-0.792843000	4.369287000	-0.437187000
C	-0.162381000	-1.146524000	-2.321969000
H	0.815057000	-1.375284000	-2.761186000
H	-0.645128000	-0.410451000	-2.971938000
C	5.317149000	-2.310802000	1.280504000
H	5.539439000	-3.332530000	1.570918000
C	-1.932077000	-1.533867000	2.813217000
C	3.997498000	-1.882120000	1.206639000
H	3.194464000	-2.576898000	1.443967000
C	-4.170114000	4.537498000	-0.142182000
H	-4.990146000	5.236623000	-0.271562000
C	-1.742973000	-2.698567000	2.061940000
H	-0.775644000	-3.197354000	2.082767000
C	4.751060000	0.314741000	0.524568000
H	4.534499000	1.336623000	0.224968000
C	-3.383579000	2.334376000	0.441734000
H	-3.590188000	1.317077000	0.769743000
C	-2.863907000	4.947062000	-0.393201000
H	-2.663031000	5.962946000	-0.717089000
C	-0.748795000	-0.870471000	3.484448000
H	-1.067651000	-0.291845000	4.364352000
H	-0.047066000	-1.631341000	3.838455000
C	6.072144000	-0.115833000	0.608787000
H	6.879386000	0.571049000	0.376896000
C	-0.419889000	-3.680198000	-1.707233000
H	0.649216000	-3.732497000	-1.944152000
C	-4.430863000	3.231991000	0.273897000
H	-5.451122000	2.916307000	0.467226000
C	-3.194341000	-0.938757000	2.817260000
H	-3.377578000	-0.062754000	3.435935000

3[κ³]⁺:

Mn	-0.265328000	0.520033000	-1.000409000
P	0.915971000	1.354922000	0.806671000
P	-1.614063000	-0.610497000	-2.438632000
P	1.403742000	0.089458000	-2.473483000
P	-1.717521000	0.590552000	0.799893000
N	0.032892000	-1.041749000	-4.548631000
N	0.266838000	-1.790277000	-1.028088000
C	-0.637492000	2.113014000	-1.679672000
C	-0.590465000	1.600103000	1.868045000
O	-0.869843000	3.107878000	-2.237276000
C	-2.000212000	-0.981948000	1.688578000
C	2.105648000	0.349466000	1.768132000
C	1.735719000	2.996228000	0.759848000
C	-0.931874000	-2.206420000	-1.805883000
C	1.483756000	-1.653853000	-1.875173000
C	3.098188000	0.743115000	-2.437184000
C	-3.341623000	1.435497000	0.837157000
C	-3.426191000	-0.620065000	-2.301598000
C	1.031686000	-0.030918000	-4.289361000
C	-2.921560000	-1.888725000	1.153702000
C	-1.331778000	-0.667373000	-4.278893000
C	2.053291000	0.167685000	3.152634000
C	-3.441880000	2.634017000	0.129211000
C	3.142879000	-0.246366000	1.051293000
C	0.984969000	4.094087000	0.338942000
C	0.923421000	-4.122154000	-0.242754000
C	3.298915000	2.103080000	-2.179655000
C	0.519521000	-2.707856000	0.112311000
C	-5.692588000	1.595625000	1.362944000
C	3.099526000	3.163676000	1.005083000
C	-5.557926000	-1.709415000	-1.950304000
C	-4.654867000	3.303434000	0.042144000
C	-1.184683000	-1.404152000	2.735166000
C	4.090525000	-1.035152000	1.698237000
C	-3.006028000	-3.184874000	1.648183000
C	3.694089000	4.405050000	0.816289000
C	1.320165000	-2.984424000	-5.238205000
C	-2.163169000	-3.613938000	2.670063000
C	-5.791690000	2.784938000	0.650791000
C	-1.255641000	-2.711704000	3.207886000
C	-4.179109000	-1.786655000	-2.127342000
C	5.685187000	1.777254000	-2.289091000
C	0.871103000	-4.110063000	-4.540933000
C	2.988132000	-0.637335000	3.790060000
F	4.766564000	-2.155744000	-0.262729000
C	4.009315000	-1.249548000	3.066687000
F	-4.123555000	-5.265786000	1.679260000
C	-4.476663000	0.927262000	1.467831000
F	-5.171278000	-3.578007000	0.811987000
C	-4.080253000	0.616963000	-2.348970000
C	2.944193000	5.498114000	0.392336000
C	4.203746000	-0.091976000	-2.649187000
C	4.590847000	2.618906000	-2.114069000
F	-7.524706000	0.160989000	1.065782000
C	0.322980000	-1.934565000	-5.675892000
C	1.584358000	5.335547000	0.160302000

3[κ$^3_{agostic}$]$^+$:

Mn	0.101173000	-0.531129000	-0.696482000
P	1.080126000	0.778654000	0.943579000
P	-1.016225000	-1.859433000	-2.158019000
P	1.824666000	-1.945217000	-1.213119000
P	-1.589011000	0.758221000	0.241755000
N	1.068783000	-2.909443000	-3.661194000
N	-0.101708000	-3.768304000	-0.331847000
C	0.438718000	0.606149000	-2.005997000
C	-0.534666000	1.358540000	1.657257000
O	0.637020000	1.296007000	-2.918195000
C	-3.124475000	0.134648000	1.010867000
C	2.083104000	0.160337000	2.344416000
C	1.991683000	2.271735000	0.426229000
C	-1.094862000	-3.575924000	-1.373178000
C	1.278198000	-3.705652000	-0.771629000
C	3.499578000	-1.738044000	-0.518195000
C	-2.133181000	2.301244000	-0.581909000
C	-2.695843000	-1.477587000	-2.754751000
C	2.138117000	-2.149014000	-3.036241000
C	-3.760477000	-0.974138000	0.455844000
C	-0.179025000	-2.184363000	-3.790863000
C	1.596286000	-0.933740000	3.053389000
C	-1.169475000	3.240315000	-0.943736000
C	3.368471000	0.629286000	2.623425000
C	2.843537000	2.147169000	-0.668424000
C	-1.515443000	-3.372860000	1.702208000
C	4.418182000	-0.912105000	-1.179647000
C	-0.318664000	-2.997381000	0.855474000
C	-3.816568000	3.687258000	-1.614240000
C	1.877721000	3.509259000	1.063335000
C	-4.952845000	-2.104574000	-3.357477000
C	-1.529042000	4.402306000	-1.616013000
C	-3.649901000	0.713761000	2.167761000
C	4.140143000	0.002870000	3.593709000
C	-4.905126000	-1.498050000	1.044292000
C	2.580161000	4.606836000	0.579088000
C	2.559692000	-4.577300000	-4.689164000
C	-5.419810000	-0.931076000	2.202241000
C	-2.854262000	4.633527000	-1.958842000
C	-4.784166000	0.173274000	2.762177000
C	-3.670231000	-2.461861000	-2.952827000
C	6.012514000	-1.210905000	0.604120000
C	2.245461000	-5.724382000	-3.953950000
C	2.378603000	-1.565910000	4.012442000
F	6.403084000	-0.545375000	3.905355000
C	3.655411000	-1.100425000	4.292147000
F	-6.251719000	-3.411147000	1.322479000
C	-3.467287000	2.532587000	-0.922833000
F	-6.467795000	-2.302112000	-0.519809000
C	-3.011676000	-0.138825000	-3.016201000
C	3.426758000	4.479239000	-0.519220000
C	3.859906000	-2.301218000	0.710915000
C	5.661171000	-0.640304000	-0.616159000
F	-5.394111000	3.555115000	-3.349148000
C	1.501118000	-3.526557000	-4.924520000
C	3.564468000	3.240278000	-1.131367000

3[κ^2]$^+$:

C	0.259273000	-2.052384000	1.406664000
Mn	0.126723000	-1.065902000	-0.047599000
P	2.032264000	-1.920183000	-0.956902000
P	-0.867582000	-2.762097000	-1.169547000
P	0.844062000	0.844540000	1.082271000
P	-1.747932000	0.027641000	0.698309000
F	-1.219925000	4.773803000	-2.219764000
F	-1.694773000	5.467341000	-0.229551000
F	-0.355250000	6.621077000	-1.485006000
F	4.995860000	4.163750000	0.643939000
F	4.721676000	4.340745000	-1.492931000
F	4.323417000	6.038956000	-0.213385000
F	-6.062328000	4.021501000	-0.339529000
F	-4.401605000	4.670662000	0.886670000
F	-4.595828000	5.385074000	-1.152608000
F	-1.981840000	1.958617000	-4.696264000
F	-4.138434000	2.023520000	-4.829657000
F	-3.132044000	0.155635000	-4.377893000
F	-7.513573000	-0.169874000	2.186894000
F	-6.989035000	-0.772147000	0.176981000
F	2.232395000	2.719682000	6.345145000
F	4.142441000	-2.736470000	3.066528000
F	4.614639000	-2.127296000	5.091980000
F	5.856266000	-1.470507000	3.453335000
N	0.395265000	-1.255292000	-3.015477000
C	-0.592180000	-2.339050000	-2.955338000
H	-0.294195000	-3.227532000	-3.534616000
H	-1.527591000	-1.965744000	-3.379731000
C	-0.083712000	-4.440348000	-0.976452000
H	-0.111930000	-4.720539000	0.091476000
H	-0.706707000	-5.156893000	-1.520606000
N	1.256658000	-4.470330000	-1.533834000
C	3.670314000	-1.173294000	-0.675776000
C	3.855811000	0.151799000	-1.095056000
H	3.065936000	0.682186000	-1.626328000
C	5.055383000	0.806577000	-0.840786000
H	5.190821000	1.827954000	-1.181771000
C	6.072101000	0.153757000	-0.145334000
H	7.004337000	0.668874000	0.063118000
C	5.892407000	-1.159417000	0.277322000
H	6.679217000	-1.670152000	0.821328000
C	4.698433000	-1.825586000	0.008270000
H	4.576875000	-2.847262000	0.354551000
C	1.763545000	-1.732738000	-2.771246000
H	2.459849000	-0.968118000	-3.115664000
H	1.992727000	-2.666732000	-3.305042000
C	2.259595000	-3.748612000	-0.761466000
H	3.242779000	-4.009008000	-1.163587000
H	2.246422000	-4.014528000	0.310250000
C	1.702407000	-5.833158000	-1.863572000
H	0.866548000	-6.333852000	-2.363932000
H	1.929493000	-6.413708000	-0.952897000
C	2.899735000	-5.813015000	-2.783666000
C	4.139111000	-6.298149000	-2.369539000
H	4.244081000	-6.724099000	-1.374330000
C	5.242113000	-6.243935000	-3.220814000

4[κ^3]$^+$:

H	-1.548658000	0.238697000	3.730984000
C	-3.852062000	2.586239000	1.191811000
C	-2.825703000	2.408317000	-1.382216000
C	-0.173596000	1.986353000	2.819883000
C	3.768348000	1.165385000	-2.187852000
C	-4.599617000	-1.723899000	-2.755496000
H	0.453404000	2.630814000	2.204941000
H	-0.044926000	2.270810000	3.874775000
H	-1.213559000	2.146300000	2.538883000
C	2.803871000	-1.021731000	-2.435893000
H	3.742583000	2.181675000	-1.812220000
C	4.279461000	-1.650686000	0.344287000
C	2.674198000	2.670419000	0.459192000
C	-1.861931000	-2.094263000	-2.571960000
H	-0.368934000	3.133516000	-0.966179000
C	-0.861506000	-3.311298000	3.141660000

C	-2.942482000	-1.683292000	2.193725000
P	1.291730000	0.637797000	-0.846632000
Mn	0.249069000	-0.808507000	0.661255000
C	0.537027000	3.328986000	-0.406531000
H	1.814651000	0.404627000	4.015616000
H	3.470312000	1.939403000	0.569684000
H	2.026230000	-1.746889000	-2.220179000
H	-2.821582000	0.744806000	1.569471000
C	-3.035440000	1.515677000	0.839255000
C	-3.754986000	-1.187018000	3.218710000
C	2.409494000	-2.454746000	3.179802000
C	2.741648000	0.267203000	-1.903885000
H	-0.141435000	-0.636669000	4.339390000
C	-0.659224000	-0.316818000	3.426999000
H	-0.793224000	-2.268102000	-2.511079000
F	-4.676960000	3.898751000	2.965861000
C	6.364160000	-0.442683000	0.266800000
C	0.667700000	4.562873000	0.223541000
C	1.797233000	4.862663000	0.976112000
F	3.909056000	3.392749000	3.081118000
C	-3.838105000	-0.860282000	-1.977514000
H	1.892241000	5.821737000	1.471639000
H	-4.331268000	-0.058399000	-1.440761000
C	-2.457014000	-1.039799000	-1.880709000
C	1.634556000	0.405363000	2.931312000
C	1.533893000	2.362059000	-0.286528000
H	1.994225000	-3.958038000	1.685836000
C	-2.497570000	1.427005000	-0.441390000
C	3.814134000	-0.803103000	1.354921000
H	2.175788000	1.255076000	2.511362000
O	0.702364000	-3.337454000	-0.749214000
H	-0.345435000	1.633539000	-2.522335000
H	0.042876000	-0.068251000	-2.783321000
C	-0.137955000	0.688394000	-2.013119000
C	0.497504000	-2.303846000	-0.253415000
N	0.202823000	0.580134000	2.603413000
P	-1.392669000	0.015642000	-0.818135000
P	2.128441000	-1.104205000	1.988246000
P	-1.113271000	-1.716209000	2.294143000
C	4.847170000	0.767136000	-2.972426000

5[κ³]⁺:

C	-3.421077000	-0.516632000	-0.198708000
C	-1.709342000	1.743515000	0.174736000
N	-0.022475000	-1.441294000	-1.699978000
C	6.274885000	-0.896952000	0.480514000
C	1.586336000	4.428255000	-0.689226000
C	5.707050000	0.343055000	0.755057000
C	-6.103748000	-1.316085000	-0.187452000
C	-1.982883000	4.048305000	-0.487206000
C	-1.990433000	4.433785000	0.851334000
C	-4.379816000	0.233185000	0.490276000
C	4.140637000	-1.693115000	-0.310588000
C	1.414147000	2.413368000	0.620475000
C	-0.325812000	-2.621845000	-2.524050000
C	1.358439000	-0.957616000	-1.937411000
C	0.128534000	-1.010702000	2.246849000
C	4.359471000	0.571336000	0.494609000
C	-1.856281000	2.705420000	-0.827178000
C	1.866475000	2.280422000	-1.748907000
C	5.489382000	-1.913644000	-0.055678000
C	-1.701338000	2.136750000	1.517870000
C	-1.853430000	3.477812000	1.854600000
C	1.653295000	1.643491000	-0.522616000
C	1.391829000	3.800946000	0.538386000
C	-5.155852000	-2.067805000	-0.876686000
C	-3.823692000	-1.672298000	-0.877795000
C	-5.712455000	-0.168718000	0.494910000
C	3.562343000	-0.446428000	-0.040998000
C	1.819931000	3.668497000	-1.832397000
C	-1.023663000	-0.340845000	-1.889807000
C	-1.279364000	-2.777548000	0.815437000
C	1.226999000	-2.892491000	0.708030000
H	-2.089101000	4.793320000	-1.269061000
H	-2.105049000	5.481175000	1.112222000
H	-1.584675000	1.395798000	2.304740000
H	-1.860409000	3.774847000	2.898503000
H	1.244936000	1.928495000	1.578212000
H	6.313787000	1.141668000	1.169400000
H	3.938982000	1.549563000	0.702292000
H	3.555013000	-2.509838000	-0.719542000
H	-5.451420000	-2.964949000	-1.410808000
H	-7.144021000	-1.624877000	-0.182996000
H	-3.101362000	-2.281850000	-1.412436000
H	5.924139000	-2.883439000	-0.274618000
H	-1.883737000	2.417731000	-1.874223000
H	1.207508000	4.390037000	1.430298000
H	1.559538000	5.511306000	-0.754742000
H	1.982699000	4.156529000	-2.788036000
H	2.090738000	1.706584000	-2.643210000
H	7.326775000	-1.071489000	0.682112000
H	-0.269591000	-2.388941000	-3.595651000
H	0.386642000	-3.415419000	-2.288476000
H	-1.326721000	-2.988505000	-2.289746000
H	2.011803000	-1.825174000	-2.053653000
H	-0.543415000	0.552750000	-2.301547000
P	-1.653803000	-0.035969000	-0.171440000
Mn	0.024721000	-1.534170000	0.506666000
O	-2.057033000	-3.589052000	1.037521000
H	-4.098954000	1.138718000	1.017223000
H	-6.446544000	0.423530000	1.031564000
H	-1.811980000	-0.649651000	-2.581539000
H	1.446119000	-0.351666000	-2.847982000
O	0.201077000	-0.595315000	3.314119000
O	1.912121000	-3.799134000	0.866411000
P	1.777462000	-0.157861000	-0.319745000

Analysis of Mn^{I}-N(sp^3) Distances in the Cambridge Structural Database

Entry	Mn-N distance	Fragment #
BEFPOR	2.096	1
FAZTEG	2.215	1
FAZTOQ	2.21	1
HIJHEN	2.077	1
ISURIY	2.236	1
KOZPOE	2.159	1
KOZPOE	2.151	2
MAMPMN	2.139	1
NAKWIG	2.211	1
NAKWIG01	2.222	1
NAKWIG01	2.225	2
NAKWOM	2.175	1
NAKWOM	2.186	2
NAKWOM	2.212	3
NAKWUS	2.209	1
NAKXAZ	2.196	1
NAKXIH	2.195	1
NAKXON	2.211	1
QIHQIH	2.208	1
QIHQIH	2.069	2
RIFFAN	2.156	1
RIFFER	2.148	1
RIFFER	2.16	5
SICFAM	2.133	1
SICFEQ	2.138	1
TAMDAM	2.102	1
TAMDIU	2.144	1
UCAKIU	2.109	1
UCAKIU	2.118	2
YIYLEX	2.148	1
YUWFOL	2.18	1

Average: 2.166 Å
Median: 2.160 Å
St Dev: 0.046 Å

References.

1. Connelly, S. J.; Kaminsky, W.; Heinekey, D. M., *Organometallics* **2013,** *32*, 7478-7481.

2. Hulley, E. B.; Welch, K. D.; Appel, A. M.; DuBois, D. L.; Bullock, R. M., *J. Am. Chem. Soc.* **2013,** *135*, 11736-11739.

3. Welch, K. D.; Dougherty, W. G.; Kassel, W. S.; DuBois, D. L.; Bullock, R. M., *Organometallics* **2010,** *29*, 4532-4540.

4. Franz, J. A.; O'Hagan, M.; Ho, M.-H.; Liu, T.; Helm, M. L.; Lense, S.; DuBois, D. L.; Shaw, W. J.; Appel, A. M.; Raugei, S.; Bullock, R. M., *Organometallics* **2013,** *32*, 7034-7042.

5. Wilson, A. D.; Fraze, K.; Twamley, B.; Miller, S. M.; DuBois, D. L.; Rakowski DuBois, M., *J. Am. Chem. Soc.* **2008,** *130*, 1061-1068.

6. Frisch, M. J.; Trucks, G. W.; Schlegel, H. B.; Scuseria, G. E.; Robb, M. A.; Cheeseman, J. R.; Scalmani, G.; Barone, V.; Mennucci, B.; Petersson, G. A.; Nakatsuji, H.; Caricato, M.; Li, X.; Hratchian, H. P.; Izmaylov, A. F.; Bloino, J.; Zheng, G.; Sonnenberg, J. L.; Hada, M.; Ehara, M.; Toyota, K.; Fukuda, R.; Hasegawa, J.; Ishida, M.; Nakajima, T.; Honda, Y.; Kitao, O.; Nakai, H.; Vreven, T.; Montgomery Jr., J. A.; Peralta, J. E.; Ogliaro, F.; Bearpark, M. J.; Heyd, J.; Brothers, E. N.; Kudin, K. N.; Staroverov, V. N.; Kobayashi, R.; Normand, J.; Raghavachari, K.; Rendell, A. P.; Burant, J. C.; Iyengar, S. S.; Tomasi, J.; Cossi, M.; Rega, N.; Millam, N. J.; Klene, M.; Knox, J. E.; Cross, J. B.; Bakken, V.; Adamo, C.; Jaramillo, J.; Gomperts, R.; Stratmann, R. E.; Yazyev, O.; Austin, A. J.; Cammi, R.; Pomelli, C.; Ochterski, J. W.; Martin, R. L.; Morokuma, K.; Zakrzewski, V. G.; Voth, G. A.; Salvador, P.; Dannenberg, J. J.; Dapprich, S.; Daniels, A. D.; Farkas, Ö.; Foresman, J. B.; Ortiz, J. V.; Cioslowski, J.; Fox, D. J. *Gaussian 09*, Gaussian, Inc.: Wallingford, CT, USA, 2009.

7. Chai, J.-D.; Head-Gordon, M., *PCCP* **2008,** *10*, 6615-6620.

8. Andrae, D.; Häußermann, U.; Dolg, M.; Stoll, H.; Preuß, H., *Theor. Chim. Acta* **1990,** *77*, 123-141.